



# Generation of colorectal cancer organoids as a preclinical model

Bachelor's Degree in Biotechnology – Academic Year: 2019/2020

Escola Tècnica Superior de Enginyeria Agronòmica i del Medi Natural - Universitat Politècnica de València

**Author:**

Lucía López Gil

**Tutor:**

Josefa Castillo Aliaga

**Collaborating external cotutor:**

Andrés Cervantes Ruipérez

**Tutor UPV:**

Máximo Ibo Galindo Orozco

Valencia, June 2020



**TITLE:** Generation of colorectal cancer organoids as a preclinical model

**SUMMARY:** Cell lines and animal models are the most common systems used for cancer research for many years. However, these model systems are not able to perfectly represent the characteristics of the different tumors that may be encountered in each patient. To overcome such limitations, organoids are generated and used as research models, as they are able to replicate the architecture, morphology, genetic profile and, phenotypes displayed by tumors in a patient-specific way. In 2020, the Spanish Society of Medical Oncology shows that colorectal cancer (CRC) is the 4th most common type of cancer in a population. Hence, the generation of CRC organoids is expected to become one of the most promising scientific resources in the understanding of this cancer and its treatment.

In this work, a protocol for the generation of organoids is established. The organoids are derived from healthy tissue, localized tumors, colon metastasis and rectum tissue from colorectal cancer patients, using tissue biopsies. Firstly, an assay for the optimization of the current protocol is carried out, to test the percentage of Matrigel more suitable for the growth and survival of the organoids. Using the more suitable protocol, different lines are established: 2 organoid lines from localized tumor tissue and 2 organoid lines from non-tumoral tissue associated with the localized tumors previously mentioned. 1 organoid line from metastatic colorectal cancer and 2 organoid lines from rectum tissue are also established. Then, these organoids are passaged up to the constitution of culture with stable growth. They are characterized from a morphological and molecular point of view as it is necessary to verify that they are identical models to the tumor from which they are derived. There is a wide array of different assays that can be performed with the organoids; in this work, a drug assay is carried out with the objective of assessing the sensitivity of the organoids to specific drugs and comparing their response to the one observed in the patients from which they are obtained. If this works out well, it is highly possible that in the near future organoids can be used to predict the response of the patient to a specific treatment, henceforth focusing on precision medicine. Finally, the organoids, that are established, have become part of a biobank generated by the research team in which I collaborated.

**KEYWORDS:** Organoids; colorectal cancer; tissue biopsy; morphological characterization; genetic analysis; precision medicine

**AUTHOR:** Lucía López Gil

**TUTOR:** Josefa Castillo Aliaga

**COLLABORATING EXTERNAL COTUTOR:** Andrés Cervantes Ruipérez

**TUTOR UPV:** Máximo Ibo Galindo Orozco

**Valencia, June 2020**

**TÍTULO:** Establecimiento de organoides de cáncer colorrectal como modelo preclínico

**RESUMEN:** Las líneas celulares y los modelos animales son los sistemas más utilizados en la investigación sobre cáncer y lo han sido durante muchos años. Sin embargo, estos sistemas modelo no son capaces de representar a la perfección las características de los diferentes tumores que podemos encontrar en los pacientes. Así pues, para poder superar dichas limitaciones, se han generado los organoides como modelos preclínicos de la enfermedad, ya que éstos son capaces de replicar aspectos como la arquitectura, morfología, perfil genético y fenotipo asociados a los tumores estudiados de manera paciente-específica. La Sociedad Española de Oncología Médica, en el año 2020, muestra como el cáncer colorrectal (CCR) es el 4º tipo de cáncer más común en la población global. La generación de organoides de CCR se prevé que pueda posicionarse como uno de los recursos científicos más prometedores para comprender este tipo de cáncer, así como su tratamiento.

En este trabajo se han generado organoides derivados de tejido sano, tumores localizados, así como metástasis y recto, de pacientes afectados por cáncer colorrectal, a partir de biopsias tisulares. En primer lugar, se ha realizado un ensayo para la optimización del protocolo actual en el que se ha comprobado cuál era el porcentaje de Matrigel más adecuado para el crecimiento y supervivencia de los organoides. Utilizando el procedimiento más óptimo se han podido establecer 2 líneas de organoides tumorales procedentes de cáncer colorrectal localizado y 2 líneas de la parte no tumoral pareada. También se ha establecido 1 línea de organoides de cáncer colorrectal metastásico y 2 líneas de organoides de recto. Estos organoides se han amplificado hasta obtener un cultivo con crecimiento estable. Se ha realizado la caracterización tanto a nivel molecular como morfológico, ya que es necesario verificar que son modelos idénticos al tumor del que provienen. Entre la gran variedad de ensayos que se pueden llevar a cabo, en el trabajo se ha realizado un ensayo de drogas con el objeto de evaluar la sensibilidad frente a diferentes fármacos y comparar la respuesta del organoide con la respuesta del paciente del que proceden. Si esto es así en un futuro los organoides pueden ser utilizados para predecir la respuesta de los pacientes a determinados tratamiento acercándonos a una medicina de precisión. Finalmente, destacar que los organoides establecidos en este proyecto han pasado a formar parte de un biobanco generado por el equipo de investigación con el que he colaborado.

**PALABRAS CLAVE:** Organoides; cáncer colorrectal; biopsia tisular; caracterización morfológica; análisis genético; medicina de precisión

**AUTOR:** Lucía López Gil

**TUTOR:** Josefa Castillo Aliaga

**COTUTOR EXTERNO COLABORADOR:** Dr. Andrés Cervantes Ruipérez

**TUTOR UPV:** Máximo Ibo Galindo Orozco

**Valencia, Junio 2020**

## **ACKNOWLEDGMENTS**

La primera a la que agradecer y la más importante de todas las personas que me han ayudado en este trabajo ha sido mi tutora Pepa Castillo. Quiero darle las gracias por dar el 120% para que este trabajo estuviera perfecto. Le ha dedicado horas y horas todos los días, tanto durante la semana como en los fines de semana, por la mañana y por las noches. Siempre animándome y dándome consejos de cómo mejorar lo que había escrito, cómo enfocarlo para que fuera más interesante... He tenido mucha suerte en encontrar una tutora tan dedicada. No te lo he dicho lo suficiente, pero te agradezco muchísimo lo que has hecho por mí durante mi estancia en el laboratorio y durante estas semanas de correcciones.

En segundo lugar, quiero dar las gracias a todos los que formáis el laboratorio 3, donde he aprendido muchísimo de la vida en el laboratorio. Hacer mi trabajo con vosotros ha sido una experiencia increíble. A Fernanda por ayudarme a diseñar los experimentos de este trabajo, proponerme nuevas ideas y supervisar que lo estaba haciendo bien. También por aguantar y responder los miles de correos preguntándole todas las dudas que me surgían, y dándome ánimos en todo momento. A Federica, por enseñarme como desenvolverse en un laboratorio nuevo, explicarme todas mis dudas de forma clara, responder a mis correos super rápido y por dejarme seguirla a todas partes, sobre todo durante las primeras semanas. Viéndote he aprendido muchísimo. A Manuel, Zahara, Blanca y Ana por enseñarme nuevas técnicas y ayudarme a mejorar este trabajo sobre todo en cuanto a detalles de los procedimientos y los materiales. Finalmente, agradecer a Andrés Cervantes por ver potencial en mí y acogerme en su grupo de investigación. He tenido mucha suerte al trabajar en este grupo.

A mis amigas de toda la vida porque nos ha tocado sufrir una pandemia y el TFG al mismo tiempo, pero lo hemos sacado adelante. A todos los amigos que he hecho en la universidad porque habéis hecho mas llevaderos los exámenes, las horas interminables de laboratorio, las trescientas nuevas tareas que nos tocaba hacer en cada asignatura y los trabajos en grupo. Las clases nunca eran aburridas con vosotros. Finalmente, le doy las gracias a mi familia por escucharme hablar únicamente de este trabajo durante semanas y apoyarme en todo momento. Sin ellos no habría llegado tan lejos.

## **CONTENTS**

<b>1.</b>	<b>INTRODUCTION</b> .....	<b>1</b>
1.1.	Colorectal cancer.....	1
1.2.	Current treatments for localized and metastatic CRC.....	3
1.3.	Preclinical models in cancer research.....	5
1.4.	Organoids as preclinical models in cancer.....	6
1.4.1.	Definition.....	7
1.4.2.	Applications in cancer research.....	7
1.4.3.	Organoid biobanking: a tool in personalized medicine.....	10
1.4.4.	Advantages and limitations of organoids.....	10
1.4.5.	New applications.....	11
<b>2.</b>	<b>OBJECTIVES OF THE BACHELOR'S thesis (TFG)</b> .....	<b>12</b>
<b>3.</b>	<b>MATERIALS &amp; METHODS</b> .....	<b>13</b>
3.1.	Recruiting patients, asking for informed consent and sample collection.....	13
3.2.	Generation of organoids.....	13
3.3.	Monitorization of organoids using optical microscopy.....	15
3.4.	Organoid passaging.....	15
3.5.	Organoid cryopreservation.....	15
3.6.	Thawing of cryopreserved organoids.....	16
3.7.	Paraffin embedding and Hematoxylin & Eosin staining.....	16
3.8.	Immunohistochemistry.....	16
3.9.	Immunofluorescence.....	17
3.10.	Genomic DNA extraction.....	17
3.11.	Genetic sequencing using a customized panel.....	18
3.12.	Drug assay.....	18
<b>4.</b>	<b>RESULTS &amp; DISCUSSION</b> .....	<b>20</b>
4.1.	<b>OBJECTIVE 1</b> Fine-tuning the protocol for the generation and growth of the organoids by finding the most suitable percentage of Matrigel.....	20
4.1.1.	Growth rate.....	20
4.1.2.	Morphological evolution.....	22
4.2.	<b>OBJECTIVE 2</b> Generation and maintenance of organoids derived from: colonic tumoral and non-tumoral tissue, liver metastatic tumoral tissue and rectum tumor tissue.....	23
4.2.1.	Generation of colon tumor/peritumoral organoids.....	23
4.2.2.	Generation of metastatic colon organoids.....	24
4.2.3.	Generation of rectum organoids.....	25
4.3.	<b>OBJECTIVE 3</b> Morphological and molecular characterization of the organoids.....	26
4.3.1.	Morphological analysis of organoids.....	26
4.3.1.1.	Hematoxylin & Eosin staining.....	26
4.3.1.2.	Immunohistochemistry.....	26
4.3.1.3.	Immunofluorescence.....	28
4.3.2.	Molecular characterization by Next Generation Sequencing using a customized panel.....	29
4.4.	<b>OBJECTIVE 4:</b> Determination of the sensitivity of the generated organoids to current treatments.....	31
<b>5.</b>	<b>CONCLUDING REMARKS</b> .....	<b>34</b>
<b>6.</b>	<b>REFERENCES</b> .....	<b>35</b>
<b>7.</b>	<b>APPENDIX</b> .....	<b>39</b>

## **ABBREVIATIONS**

**APC:** Adenomatous Polyposis Coli

**aSCs:** adult Stem Cells

**BM:** Basal Medium

**CM:** Complete Medium

**CMS:** Consensus Molecular Subtypes

**CNO:** Colon Normal Organoid

**CRC:** Colorectal Cancer

**CTO:** Colon Tumor Organoid

**E-cad:** E-cadherin

**ECM:** Extracellular Matrix

**HCUV:** Hospital Clínico Universitario de Valencia

**HGVSp:** Human Genome Variation Society protein sequence name

**H&E:** Hematoxylin and Eosin staining

**LOH:** Loss of Heterozigosity

**mCTO:** metastatic Colon Tumor Organoid

**MSI:** Microsatellite instability

**MUC:** Mucin

**P/E:** Penicillin / streptomycin

**P24W:** 24-well suspension plate

**P96W:** 96-well suspension plate

**RBC:** Red Blood Cells

**RTO:** Rectum Tumor Organoid

**ST:** StemCell

**UCIM:** Unidad Central de Investigación Médica

## **FIGURES**

<b>Figure 1.</b> Estimation of new cases and deaths for several cancer types.....	1
<b>Figure 2.</b> Evolution of colorectal cancer from a precursor lesion.....	2
<b>Figure 3.</b> Categorization of CRC types based on CMS.....	3
<b>Figure 4.</b> Treatments available for patients with metastatic colon cancer.....	4
<b>Figure 5.</b> Main characteristics of current preclinical oncology models: cell lines, xenografts and organoids.....	6
<b>Figure 6.</b> Applications of normal and tumor organoids in research.....	8
<b>Figure 7.</b> Growth of organoids cultured in different Matrigel concentrations.....	21
<b>Figure 8.</b> Evaluation of organoid morphology in different culture conditions (Low, High and Medium Matrigel concentration).....	22
<b>Figure 9.</b> Generation and maintenance of CTO65-P02 (localized colon tumor organoids).....	24
<b>Figure 10.</b> Generation and maintenance of mCTO50 (metastatic colon organoids).....	24
<b>Figure 11.</b> Generation and maintenance of RTO8 (rectum organoids).....	25
<b>Figure 12.</b> H&E staining of tumoral and metastatic organoids.....	26
<b>Figure 13.</b> Immunostaining of rectum organoids.....	27
<b>Figure 14.</b> Immunofluorescence of adenoma-derived organoids (CAO29).....	28
<b>Figure 15.</b> Comparison of the effects of each monotherapy and the combined therapy on CTO65-P02 organoid viability.....	32

## **TABLES**

**Table 1.** Mutation frequency of colorectal cancer-related genes comparing CTT65 (tissue) and CTO65 (tumor organoids).....**29**

# 1. INTRODUCTION

## 1.1 Colorectal cancer

Cancer causes one out of six deaths worldwide and with the increase of aging population, it is expected to increase (World Health Organization, 2018). Colorectal cancer (CRC) is the third most common cancer in both males and females (Siegel *et al.*, 2020). It is estimated that 53.000 people will die of CRC cancer this year. Generally, it is predominantly found in rich/developed countries and continents such as North America, Europe, Australia, etc. Lifestyle factors, such as dietary habits, which include consuming high amounts of red or processed meats are among risk factors that influence CRC development (**Figure 1**).

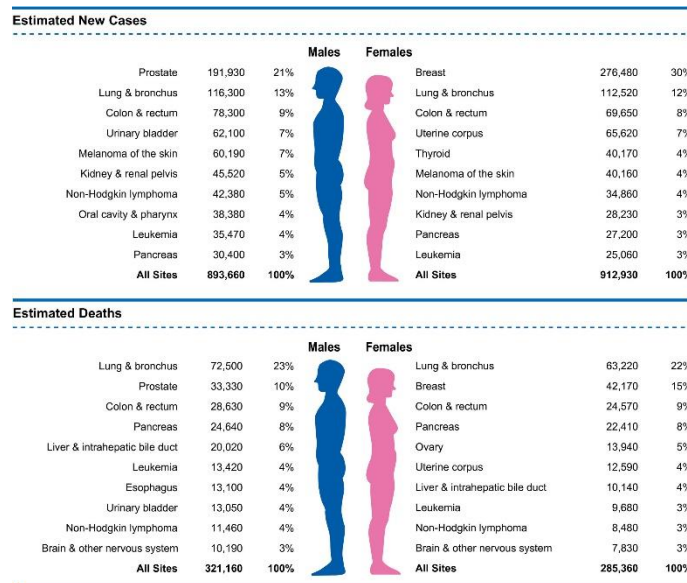


**Figure 1. Estimation of new cases and deaths for several cancer types.** Distribution was made based on sex (US, 2020). Data taken from Siegel *et al.*, 2020.

This cancer is one of the main beneficiaries of targeted therapies, mainly because there is a clear link between molecular mechanisms and the malignant phenotype. 25% of the diagnosed patients will already have metastasis, whereas 40% will develop metastasis within a year (Florescu-Tenea *et al.*, 2019). Several advances in treatment against cancer progression have flourished in the past years. However, most of them do not adequately work due to the tumor heterogeneity between and within individual patients.

### Models of colorectal cancer development

The origin of CRC tends to be a neoplastic precursor lesion, called a polyp. This begins in a colonic crypt and evolves to a fully-fledged CRC in 10-15 years (Dekker *et al.*, 2019). Cancer stem cells are believed to be the founders of CRC. These cells accumulate genetic and epigenetic mutations, leading to the activation of pro-tumorigenic pathways as well as the inactivation of the suppression of tumorigenic processes. The investigation of these cells is essential for preventive treatment as well as for choosing a therapeutic approach.

Globally, three pathways can explain the evolution of the disease from a precursor lesion (**Figure 2**). All the events tend to occur in sequential order (Cancer genome atlas network, 2012). On one hand, there is the adenoma-carcinoma pathway, also called

chromosomal instability sequence (A), which causes the majority of CRC. On the other hand, there is the serrated neoplasia pathway, (B) which represents 10-20% of the cases. In pathway A, mutations affect APC, then RAS activation, or TP53 loss-of-function occur. Conversely, pathway B is characterized by epigenetic instability due to altered methylation, which leads to microsatellite stable and unstable cancer. Genes that appear mutated in this pathway are RAS and RAF. Lastly, there is a third possible development pathway (C), which accounts for a very small percentage of the cases, characterized by microsatellite instability. This is common in Lynch syndrome (non-polyposis syndrome). Mutations affecting DNA mismatch repair genes happen in the germline cells (Nojadeh *et al.*, 2018).

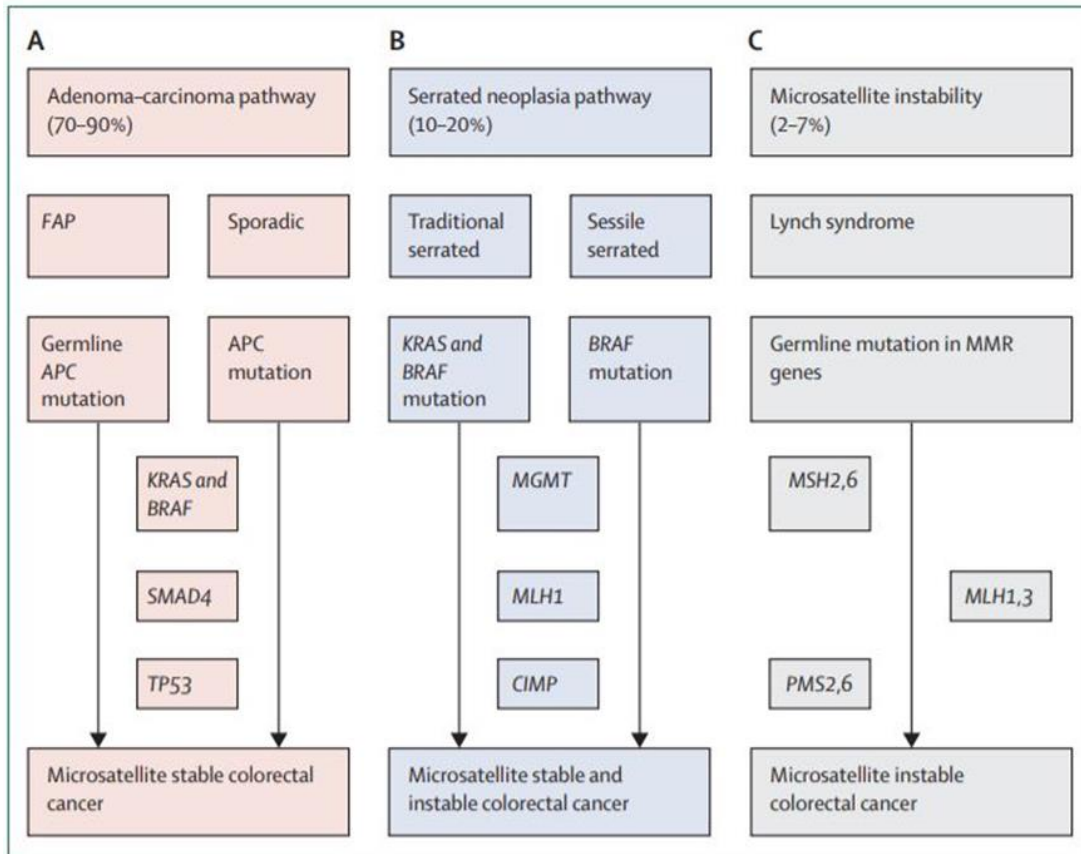


**Figure 2. Evolution of colorectal cancer from a precursor lesion.** Microsatellite stable cancers appear due to the sequential accumulation of mutations starting from APC mutations (A). Serrated neoplasia starts from KRAS/BRAF mutations and progresses acquiring a CpG island methylator phenotype (CIMP), which inhibits tumor suppressor genes (B). Lastly, in the microsatellite instability pathway, CRC development starts due to mutations affecting DNA mismatch repair genes (C). FAP: familial adenomatous polyposis. Taken from Dekker *et al.*, 2019.

## Classification of colorectal cancer

The most used classification of CRC is based on clinical-pathological criteria, using a system called TNM from the American Joint Committee on Cancer. Four stages (I-IV) are designated based on the degree of local tumoral infiltration (T), the number of affected lymph nodes (N) and metastasis (M). However, several limitations are associated with this system, especially regarding prognosis and drug response prediction. Therefore, other types of CRC cataloging, based on molecular classification, are increasingly being used.

From 2014, a new classification based on gene expression profile allowed for the establishment of four molecular subtypes (consensus molecular subtypes [CMS] 1-4)

(Guinney *et al.*, 2015). Each subtype has a unique genetic signature. Most of MSI tumors (right-sided tumors) are within the CMS-1 group (also known as MSI immune subtype). Tumors associated with chromosomal instability are within the other three subtypes: CMS2 (canonical subtype), CMS3 (metabolic subtype), and CMS4 (mesenchymal subtype). An overview of the main characteristics of each molecular subtype is summed up in **figure 3**.

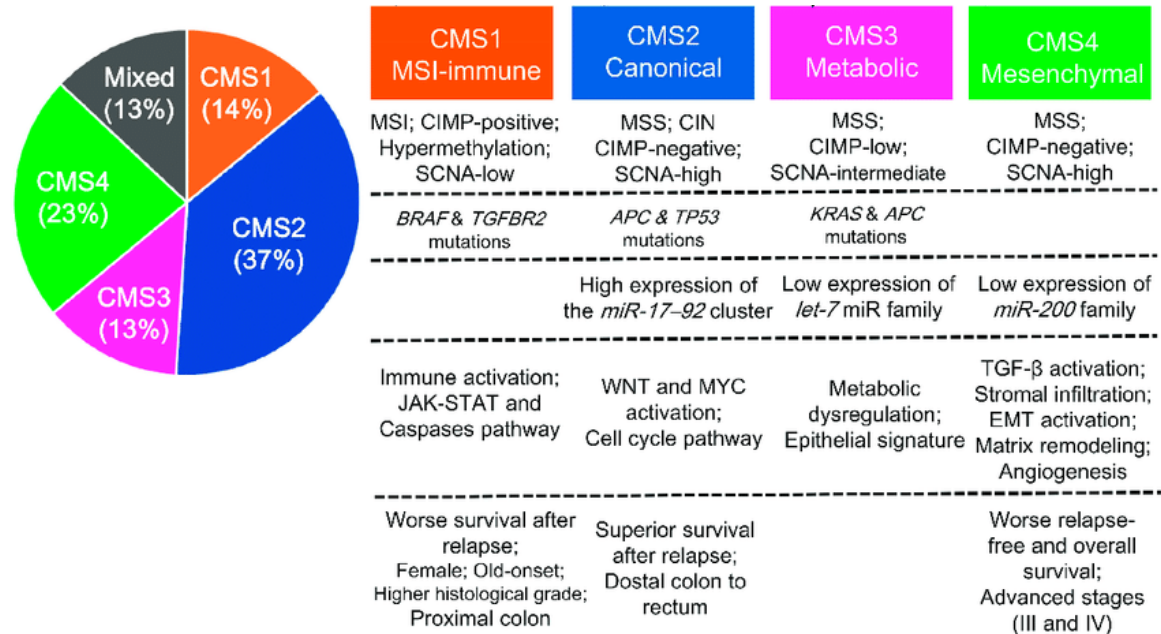


**Figure 3. Categorization of CRC types based on CMS.** The image on the left indicates the frequency of each subtype whereas the image on the right lists the main characteristics of each subtype. Some abbreviations are used: CIMP: CpG Island Methylator Phenotype; CIN: Chromosomal Instability; CMS: Consensus Molecular Subtype; MSI: Microsatellite Instability; MSS: Microsatellite Stability; SCNA: Somatic Copy Number Alteration. Image taken from Inamura, 2018.

## 1.2 Current treatments for localized and metastatic CRC

The stage at which the tumor is classified influences the treatment. The most common cancer treatments are tumor removal through surgery and radiotherapy at stages 0-III. A combination of local surgery and adjuvant chemotherapy based on fluoropyrimidines is used (with or without oxaliplatin) for stage II and more advanced stages. If the tumor is metastatic, the treatment tends to be systemic and chemotherapy is predominantly used. Lately, more innovative treatments are proposed, such as targeted agents and the ones based on the patient's immune system known as immunotherapy.

A wide range of available treatments can be further classified as (**Figure 4**):

- **Biologics/Biological-based treatments:** It is common to find that cancer cells acquire mutations that constitutively activate receptors or overexpress factors that allow the continuous proliferation and differentiation of tumoral cells. Therapies such as anti-EGFR and anti-VEGF are used. EGFR is an epidermal growth factor receptor that in its active form induces a signaling cascade triggering cellular differentiation, proliferation and the activation of anti-apoptotic proteins, whereas VEGF is a vascular endothelial growth factor that promotes angiogenesis, a key process in the tumorigenesis. Examples: Cetuximab (ERBITUX®) as an anti-EGFR and Bevacizumab (AVASTIN®) as an anti-VEGF.

- Chemotherapy: Irinotecan, Oxaliplatin, and Fluoropyrimidines (Fluorouracil) are included in this group. These agents act by disrupting DNA replication inhibiting enzymatic action or in the case of oxaliplatin by forming adducts which ultimately leads to apoptosis.

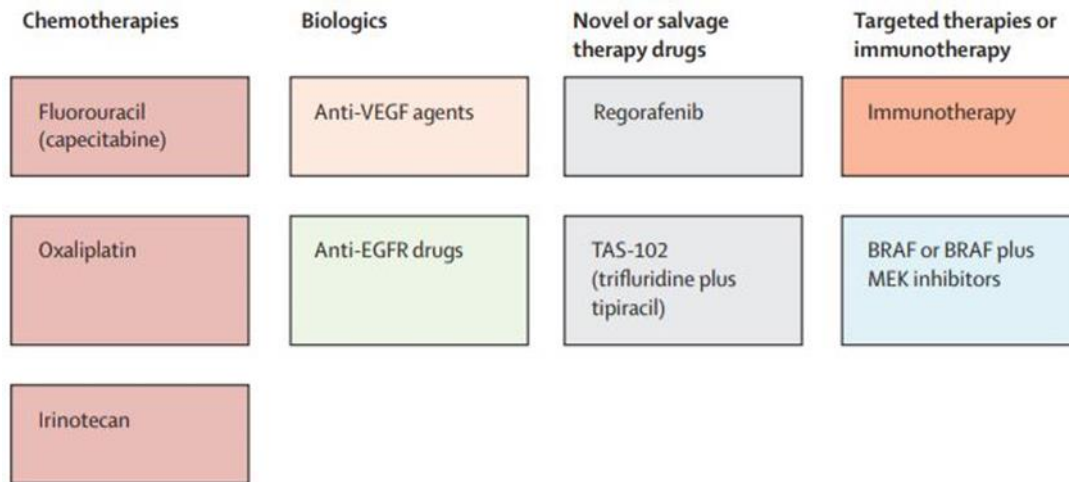


**Figure 4. Treatments available for patients with metastatic colon cancer.** Four main approaches are currently used when a treatment for advanced CRC is required. Combinations between them are possible. Image taken from Dekker *et al.*, 2019.

Despite current treatments, the survival for patients with metastatic CRC is under 15%. Almost 50% of CRC patients have a RAS mutation, which means that anti-EGFR drugs do not work. Another example is the presence of BRAF-V600E mutants within CRC cases. This mutant is very important since the prognosis becomes 2-3 times worse and systemic therapy does not work well (Roth *et al.*, 2010).

Although the new generation of targeted therapies has undoubtedly improved the therapeutic options of treating cancer there are important issues that need to be considered like the resistance of cancer cells against treatments. A better understanding of tumor cell biology in every patient could offer the possibility of attaining truly personalized drug-based therapy increasing the effectiveness.

Optimal preclinical models are essential to design adequate treatments for each patient. Molecular features have great relevance and genetic and epigenetic factors are also essential in understanding each tumor, hence there is a need for the development of reliable models to analyze the effects of the treatments.

### 1.3 Preclinical models in cancer research

Heterogeneity in cancer models is essential to have a wide view of the disease progression and evolution as well as for developing personalized treatment (Fan *et al.*, 2019). The differences between patients influence parameters such as tumor growth rate, invasion ability, or drug sensitivity (McGranahan & Swanton, 2017). Therefore, treatments should be optimized to obtain a full recovery.

Human-derived models used in cancer research include classical *in vitro* models such as immortalized cancer cell lines and *in vivo* models like patient-derived tumor xenografts (PDXs) (Sachs & Clevers, 2014). More recent tools include organoid generation. Each of these has its advantages and limitations (**Figure 5**).

Cell lines are probably the most used model in research. They are easy to maintain, and gene editing tools are used to modify them. Protocols for high-throughput screening for many treatments as well as the determination of sensitivity to drugs have already been established. The use of cell lines in cancer research has some inherent limitations such as that only a specific cell type is analyzed, not achieving the cellular diversity present in the tumors (Nagle *et al.*, 2018), and they can only be established from a limited number of cancer subtypes (Gao & Chen, 2015). Additionally, cellular and cell-matrix interactions cannot be replicated in this 2D model. This limitation was partially solved with 3D cell culture; however, the resulting structures were still lacking. 3D cell cultures or spheroids represent single components within tissue as they are derived from monoculture, they do not allow long term culture and more importantly, they do not completely recapitulate on tissue physiology. Another limitation when working with cell lines is that they can acquire mutations as time progresses, hence the heterogeneity that is present in these cell lines may be lost in long-term cultures.

In the past few years, among animal models, Patient-derived tumor xenografts (PDX) have been used. Limitations of previous models such as the lack of heterogeneity, the high genetic divergence as time in culture progresses, or the absence of the physiological environment were overcome by these *in vivo* models. PDX are generated by transplantation of patient tumoral cells into immunodeficient mice. This way it is possible to replicate the genetic and histological characteristics of the tumor for approximately 14 passages (Guenot *et al.*, 2006). This model is expensive, difficult to generate (30-40% average success rate), labor-intensive (an average of 4 months is needed) However, they are able to replicate and maintain the tumor heterogeneity in the long term preserving genomic stability during passages (Tentler *et al.*, 2012).

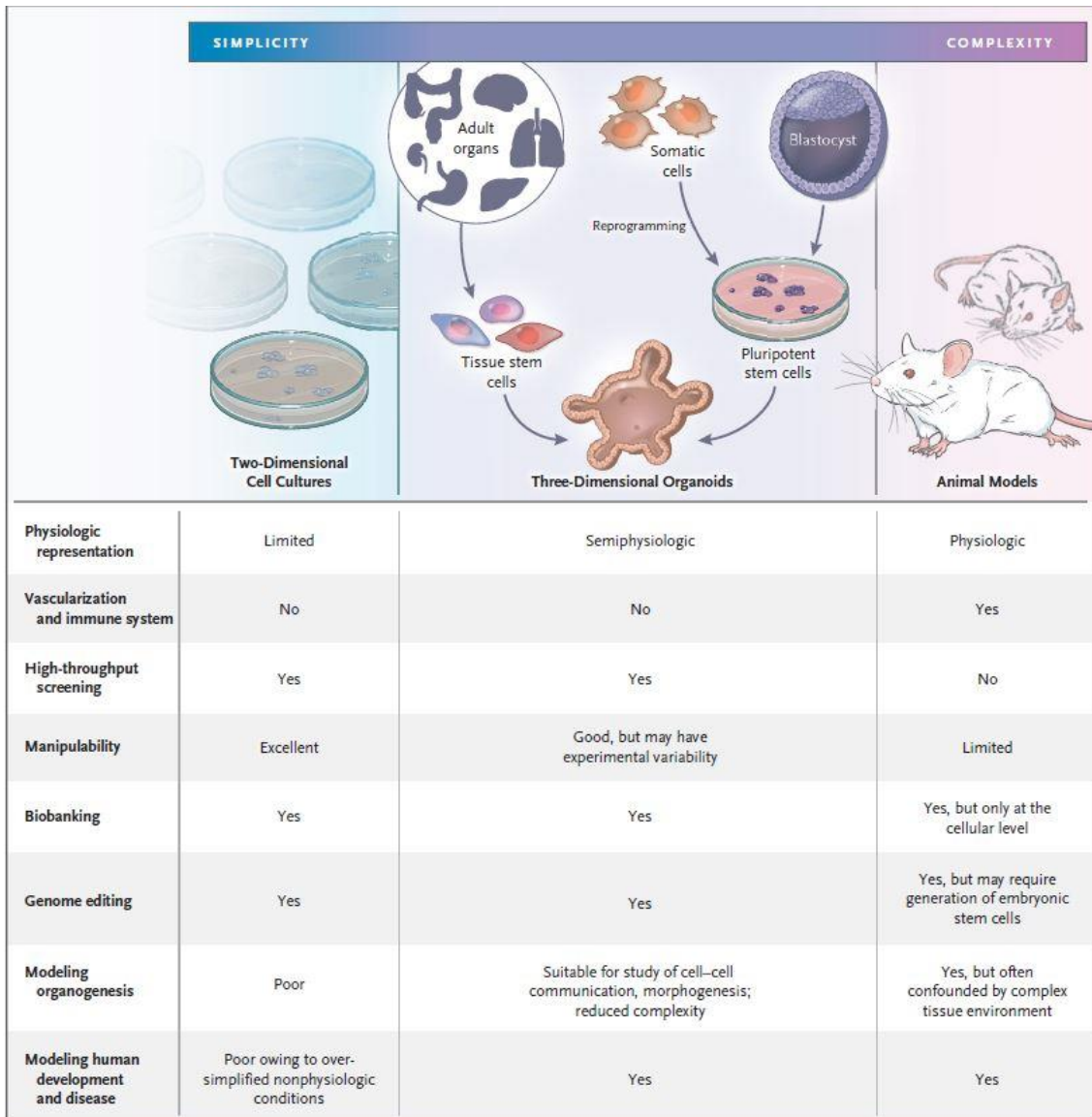


**Figure 5. Main characteristics of current preclinical oncology models: cell lines, xenografts and organoids.** Image taken from Li & Izpisua (2019)

Both cell lines and animal models have contributed greatly to cancer research, however, they present strong limitations. The number of deaths, caused by cancer, may be reduced by prevention and early detection of the disease, but current models fail to reproduce the characteristics of each tumor (Kamb, 2005), and as a consequence drugs that work on models fail when translated to patients. New preclinical models to bridge the gap between previously mentioned systems are required, and 3D organoid culture stands as a new research technique with powerful physiological relevance.

#### 1.4 Organoids as preclinical models in cancer

Recently, organoids have emerged as an alternative model that retains the heterogeneity of the primary tumor while being low-cost and easy to generate (Grandori & Kemp, 2018). Various types of patient-derived organoids have already been generated, such as liver, pancreatic, and colorectal cancer organoids (Broutier *et al.*, 2017; Boj *et al.*, 2015; Fumagalli *et al.*, 2017). A tissue biopsy can be used for the

generation of organoids from theoretically any patient, allowing an in-depth study of the mutations causing the disease. Some subclonal mutations that remained hidden when sequencing the tumor as a whole may arise through the individual analysis of organoids, and maybe it can be the key to successful treatments or to explain resistance mechanisms (Sachs *et al.*, 2018).

Importantly, it was shown that organoids can be transplanted into immunodeficient mice and conserve the characteristics of the tumor of origin (Fujii *et al.*, 2016), which may allow validation of drug response *in vivo*.

#### 1.4.1 Organoid Definition

According to Clevers (2016), an organoid is “a 3D structure developed or grown from stem cells and consisting of organ-specific cell types that self-organizes through cell sorting and spatially restricted lineage commitment”.

In general, two main types of stem cells can give rise to organoids: organ restricted adult stem cells (aSCs) or pluripotent embryonic stem cells / induced pluripotent stem cells. Organoids in cancer research are mainly derived from tissue biopsies, more specifically from the aSCs that can be found there.

Most of the aSCs-derived organoids have an epithelial nature: they are composed of highly polarized epithelium and a central lumen (Boj *et al.*, 2015; Sato *et al.*, 2011).

These stem cells are dissociated from the tissue and cultured mimicking the stem cell niche environment. The first developed organoids were intestinal (Sato *et al.*, 2009), starting from an LGR5+ intestinal stem cell. LGR5 is a receptor for R-spondin, a Wnt activator, and it acts as a marker for active aSCs (Clevers, 2016). This type of organoids needs a source of extracellular matrix to act as the basal lamina in the culture, so Basement Membrane Extract (R&D Systems) or Matrigel (Corning) are used.

Organoids can be passaged, cryopreserved, genetically altered, and remain stable in the long term. The generation of organoids from tumor samples has a success rate between 15-100%, being the prostate organoids the ones with the lowest generation efficiency (Boj *et al.*, 2015; Fujii *et al.*, 2016; Gao *et al.*, 2014)

#### 1.4.2 Applications of patient-derived organoids in cancer research

Patient-derived tumor organoids are characterized by their rapid growth and stable differentiation. Organoids are able to mimic the tumor heterogeneity, which is a crucial factor as it influences molecular response to different therapies. Applications for these types of organoids include models of tumorigenesis, metastasis and they are also used in personalized drug screening, immunotherapy, and biomarkers discovery (**Figure 6**).



### Organoids as a tool to identify molecular mechanisms of metastasis

Metastasis is the spreading of cancer cells from a localized origin (primary tumor) towards other organs. This is one of the major causes of death in cancer. In this line of study, researchers, using organoid models, have been able to identify the molecular mechanisms that lead to the initiation of collective invasion in CRC adenocarcinomas (Libanje *et al.*, 2019) and how Extracellular Matrix (ECM) also modulates the invasion (Vellinga *et al.*, 2016).

### Organoids as a potential new tool used in personalized medicine

One of the strongest points of organoids is that they are able to replicate the characteristics of the tumor of origin, including response to treatment. Standard proteomic-based assays and nucleic acid-based assays are used to characterize these models. Researchers are interested in knowing how faithful the model is, so they proceed to the characterization of the generated organoids.

Targeted sequencing of organoids and primary tumor samples show a strong correlation (Boj *et al.*, 2015; Sachs *et al.*, 2018; Gao *et al.*, 2014), which means that organoids do conserve the traits of the primary tumor.

An essential objective of using models is to have new ways of discovering drugs that work against the disease as well as try to develop drugs that work efficiently. One of the most interesting studies towards personalized treatment is from Vlachogiannis *et al.* (2018). Researchers compared the response to different therapeutics, evaluating both the response in patient-derived metastatic gastrointestinal organoids and the patient itself. The results observed in the organoid correlated with the response observed in the patient and the molecular profile of both the organoids and the tumor of origin matched, showing the huge potential of patient-derived organoids as response prediction tools.

Regarding immunotherapy, organoids are of great help as they can be used to stimulate tumor reactive T-cells. If these cells are transferred back to the patients, they may be able to kill the tumor carrying the same neo-antigens. This is also known as adoptive cell therapy. Using this strategy, Dijkstra *et al.* (2018) perform a co-culture with colon organoids derived for MSI colon carcinoma and peripheral blood lymphocytes, which lead to T-cell activation and a reduction in tumor organoid viability. Quite interestingly, matched normal organoids remain unaffected. This opens a world of possibilities for personalized immunotherapy.

Lastly, tumor biomarkers regarding prognosis can be identified comparing healthy organoid lines and tumoral organoids lines as Broutier *et al.* (2017) have discovered 30 potential biomarkers based on transcriptional differences comparing both types.

### Clinical trials based on study of organoids

As of 15/05/2020 there are 15 projects related to cancer organoids registered on the website of ClinicalTrials.gov. (3 are not yet recruiting, 1 has an unknown status, 1 is enrolling by invitation, the rest have open recruiting). Among these, 47% are interventional studies and 53% are classified as observational studies. These interventional studies are mostly focused in establishing patient-derived organoids from both primary tumor and metastases and studying their growth rate, sensitivity to drugs and prediction of the response to a treatment through organoid study. A number of different cancer types are included such as CRC, pancreatic, breast cancer, esophageal cancer, lung cancer, head and neck cancer (CLINICALTRIALS.GOV (n.d.)).

### 1.4.3 Organoid biobank: a tool in personalized medicine

The creation of organoid biobanks is one of the most pursued objectives after organoid generation. Biobanks can be established as repositories of the patient-derived tumor organoids from different subtypes and stages. These sets of organoids are histologically and genetically characterized, with matched non-tumoral organoids, if possible (Schutgens & Clevers, 2020). They are cryopreserved and passaged, constituting a long-term resource that can be used for clinical research. Moreover, organoids biobanks for rare cancer subtypes have been created. This is a big step forward in cancer research as the generation of cell lines for these types of cancer is difficult and it has limited the research. In any case, stability of the generated organoids has to be checked after each passage as to detect any new mutation that may have been acquired during the long-term storage. This is specifically important MSI CRC organoids as they are prone to acquire them.

All in all, biobanks are highly promising for precision medicine as they can become a platform to further research encompassing different genetic profiles, with the potential of performing drug screening, contributing to basic and clinical research. In the past six years, several biobanks have been created (**Appendix - Supplementary table 1**).

### 1.4.4 Advantages and limitations of organoids

The main advantages of organoids are that (1) they offer the possibility of being cultured in microplates which allows the implementation of high-throughput assays; (2) they are able to replicate the genetic alterations, gene expression and histopathology present in patients, leading to personalized drug screening (Sachs *et al.*, 2018); and (3) they require less time to be fully established (Fan *et al.*, 2019).

Nevertheless, they still have some limitations. Firstly, they offer representation of a single organ derived from a single tissue sample, hence it does not allow for multiorgan analysis of the progression of the disease. On the other hand, animal-based matrix extract is required for culture, which can suffer from batch-to-batch variability, thus affecting the experimental reproducibility (Schutgens & Clevers, 2020).

Additionally, generated organoids have mostly an epithelial nature. The absence of other physiological components such as fibroblasts, endothelial cells and blood vessels may have an impact on the reliability of the model. The tumor microenvironment, the vascularization, the immune system, all these components are present in a physiological state and influence on the response to a treatment. It can be imitated to a certain degree, either by applying hypoxic conditions or adding cytokines that can elicit an immune response, but it is not a realistic representation of what the tumor response may be. In order to overcome these limitations, co-culture with immune cells has been tested and it has been successful (Dijkstra *et al.*, 2018).

Another possible limitation is that advanced tumor-derived organoids grow more slowly than “normal” organoids, which can lead to an overgrowth of normal organoids over the tumoral ones (Drost & Clevers, 2018).

### 1.4.5 New applications

Although tumor organoids imitate critical features of the original tumor, there is still room for improvement. New approaches to overcome the current limitations have been proposed. Among those, organoid-on-a-chip is one of the most promising.

Organoids are cultured on a chip, a microfluidic device that presents the advantage of allowing the control of parameters such as oxygen, temperature and pH (Yu *et al.*, 2019). This way information about crucial traits of the native tumor such as the cellular complexity, the tumor microenvironment, and the effects that it has on the tumor can be analyzed by taking advantage of the microfluidic and microfabrication of the chip (Skardal *et al.*, 2016). Consequently, better reproducibility of current generation strategies may be achieved. The integration of organoids into this system have allowed for several studies including drug-response studies (Xu *et al.*, 2013).

In conclusion, organoids provide a better understanding of the development of the disease. They recapitulate the main characteristics of the tumors and some of the high variety of different cell subtypes within a tumor. Their response to different treatments can be correlated with the patient's response, hence opening a world of possibilities as a response prediction tool, leading towards a more personalized type of medicine. The scope and impact of organoids should be expected to increase in the coming years.

## **2. OBJECTIVES OF THE BACHELOR'S THESIS (TFG)**

**Objective 1:** Fine-tuning the protocol for the generation and growth of the organoids by finding the most suitable percentage of Matrigel

**Objective 2:** Generation and maintenance of organoids derived from: colonic tumoral and non-tumoral tissue, liver metastatic tumoral tissue and rectum tumor tissue

**Objective 3:** Morphological and molecular characterization of the organoids

**Objective 4:** Determination of the sensitivity of the generated organoids to current treatments

### **3. MATERIALS AND METHODS**

#### **3.1 Recruiting patients, asking for informed consent and sample collection**

Recruited patients belong to the *Hospital Clínico Universitario de Valencia (HCUV)* and they are under the care of oncologists from the *Instituto de Investigación Sanitaria INCLIVA*. Patients were informed in detail about how they could contribute to research by donating their biological samples. The ones that agreed, signed the corresponding informed consent. From this point on, a highly interconnected sample collection system was created, involving the participation of several professionals: oncologists, surgeons, endoscopists, pathologists and researchers. The system designed for the collection of each type of sample was established, according to the institutional regulation and legal and ethical normative (*Ley de Investigación Biomédica, de 3 de Julio; Real Decreto 1716/2011, about biobanks*). This procedure was approved by the *Comité Ético de Investigación Clínica del HCUV*.

##### Localized and metastatic colon tumor samples (liver metastasis)

Both types of samples used the same sample collection pathway. Oncologists, that collaborated with researchers, identified patients waiting for tumor removal. Once identified, and with the signed informed consent, oncologists let the surgeon know that during the surgery a piece of the fresh tumor (i.e. not in formalin) should be sent to the pathology department. After receiving the sample, the pathologist contacted the researchers. Small fragments of the tumoral / non-tumoral tissue of interest were introduced in vials with cold PBS for researchers to work with.

##### Rectum tumor samples

For this type of sample, the surgeon could identify a patient of interest when a rectoscopy took place. The surgeon extracted at least 2 samples of the tumor and introduced them in a vial with PBS and Antibiotic 2x. Once it was done, the surgeon contacted the researchers so that the sample was collected.

#### **3.2 Generation of organoids**

Samples of tumoral and surrounding non-tumoral tissue conserved in PBS were washed thoroughly with PBS so that unwanted compounds and blood were removed. Then, they were incubated with an antibiotic mix 2x (penicillin-streptomycin, 2.0% [BIOWEST L0018-100]; and primocin 200 µg/mL [Invivogen ant-pm-1]) for 30 minutes. After removing the antibiotic mix, samples were washed 2-3 times with PBS again. The content was deposited into a plate and a small region was sectioned. This segment was then cut into 4 fragments and transferred to a cryovial, which was stored at -80°C. The rest of the tissue was cut in smaller pieces, transferred into a tube containing digestion mix and incubated. Digestion mix is constituted by liberase (Roche, cat. no. 05401020001), DNase (Sigma d5025-15ku) and Y factor /ROCK inhibitor Y-27632 (BioScience, cat. no. 129830-38-2). This mixture was left in a bath at 37°C for 1 hour, with manual resuspension each 15-20 minutes.

After incubation, the suspension was filtered using a 70-µm cell strainer. The contents were recovered in a 50mL tube and centrifuged (1500 rpm, 5 minutes, 4°C). Then, the supernatant was removed. Sometimes, it was possible to observe a red halo in the pellet due to the presence of Red Blood Cells (RBC). In these cases, RBC lysis buffer called ACK Lysing Buffer (Thermo, cat. no. A1049201) was added to the tube containing the

pellet and incubated up to 4 minutes. After the incubation period finished, the tube was centrifuged (1500 rpm, 5 minutes, 4°C) and the pellet was resuspended and re-centrifuged using the same conditions as previously mentioned. After this second centrifugation, 300-500 µL of Basal Medium (BM), which composition is detailed below, was added to the tube and cells were thoroughly resuspended. The volume of BM used varies with the size of the recovered pellet; bigger pellets require higher volumes.

Cells were counted using a Neubauer chamber. Afterwards, the tube containing the cells was centrifuged again (same conditions as before). The next step was the seeding, which consisted in the creation of a solidified droplet on the bottom of each well. The number of wells used depended on the number of cells recovered. A 24 wells suspension plate (P24W; CellStar, cat. no. 662102) was pre-warmed while the droplet mixture was generated.

Each droplet (final volume 40 µL) contained approximately 250.000-300.000 cells and it was constituted by 50% cell suspension and 50% Matrigel (Corning, cat. no. 356231). The droplet mixture was generated by mixing the cell suspension and Matrigel in a proportion 1:1 and one droplet was deposited per well. Then, the plate was introduced in the incubator for 20-30 min at 37°C, which allowed droplets to solidify. After this gelation step, 500 µL of culture medium was added to each well. Depending on the type of tumor sample, one medium may be more suitable than the rest. Medium was changed every 2-3 days and passages took place depending on what it was observed during monitoring of the organoid's evolution.

#### **Composition of the culture medium used in organoid culture**

- ❑ *Basal Medium (BM)*: DMEM/F12, HEPES (10 mM), L-glutamine (2 mM), P/E (1.50%), primocin (150 µg/mL), N2 (1X) and B27 (1X).
- ❑ *Complete Medium (CM)*: BM supplemented with N-acetyl-L-cysteine (1 mM) [SIGMA A9165-25G], Nicotinamide (10 mM) [SIGMA N0636-500G], EGF (50 ng/mL) [StemCell 78006], Noggin (100 ng/mL) [StemCell 78060], A-8301 (0,5 µM) [TOCRIS 2939], SB202190 (10 µM) [TOCRIS 1264], gastrin (10 nM) [TOCRIS 3006], R-Spondin1 (500 ng/mL) [StemCell 78213.1], FGF-10 (10 ng/mL) [StemCell 78037.2] and PGE2 (10 nM) [TOCRIS 2296]. → Mostly used with colon tumor samples and metastasis.
- ❑ *StemCell Medium (ST)*: A Component, B Component, P/E (1.50%) and primocin (150 µg/mL). *The composition of the ST medium is basically Intesticult™ Organoid Growth Medium Human (StemCell Technologies, cat. no. #06010) supplemented with antibiotics.* → Used with non-tumoral samples.
- ❑ *STA Medium*: A Component from Stem Cell medium, DMEM/F12, P/E (1.50%) and primocin (150 µg/mL). → Some of the colon tumor samples grow better in this medium

ROCK Inhibitor Y-27632 was added to the medium (1µl per each 1 mL of medium). This factor inhibits anoikis, a typical form of dissociation-induced apoptosis of epithelial cells.

### **Naming the organoids**

The tumor derived organoids obtained from a colon are called CTO (Colon Tumor Organoids), the ones derived from metastatic colon tumor samples are called mCTO (metastatic Colon Tumor Organoids) and the ones derived from rectum samples are called RTO (Rectal Tumor Organoids). Non-tumoral organoids are derived from samples taken from the surroundings of the main tumoral focus, also known as the peritumoral region and these are called CNO (Colon Normal Organoids).

Most of the code names include a number assigned to each different patient and registered in our database (i.e.: CNO25 are organoids derived from patient 25). Colon tumor samples that are big enough may allow sampling in different regions, these will be named P01, P02... Metastatic samples have additional coding using S, which represents the hepatic segment from which the sample is obtained. This latter designation is mostly used by the pathologists that prepare the samples for researchers.

### **3.3 Monitorization of generated organoids using optical microscopy**

Once organoids had been generated, strict monitoring was performed thrice a week using a LEICA DMI1 microscope. Growth, morphology, survival, density within the droplet, signs of contamination were some of the studied parameters. Procedures such as passaging, freezing, morphological / molecular studies took place after monitoring the progression of generated organoids.

### **3.4 Organoid passaging**

Passaging of organoids was performed when high organoid density was observed after monitoring. First, the medium inside the wells was removed. Cold PBS was added to each well with the aim of breaking down the Matrigel droplet that contained the organoids. With the help of the pipette tip, the droplet was broken down and the cells were recovered and transferred to a tube that contained cold PBS. It was centrifuged (1500 rpm, 5 minutes, 4°C), supernatant was removed and 100 µL of TrypLE Express enzyme (Life technologies, cat. no. 12605-010) was added to the pellet to digest the organoids. The tube was then introduced in the bath, which was at 37°C, and it was left for 5 min. After this incubation, 800 µL of BM was added to inactivate the trypsin and the tube was centrifuged once again under the same conditions. Then, cells were counted to determine how many droplets could be generated. The elaboration of the droplets followed the same instructions stated in the section "Generation of organoids". Depending on the wells available on the plate, the new droplets derived from the passage were deposited on the original P24W or on a new plate.

### **3.5 Organoids cryopreservation**

The procedure for cryopreserving organoids was very similar to the one described for passaging. Same steps were performed in order to break down the droplet and digestion of the organoids. After digestion, 800 µL of BM was added to inactivate the trypsin and the tube containing the organoids was centrifuged at 1500 rpm, 4°C and for 5 minutes. Then, the supernatant was removed, and the pellet was thoroughly mixed and resuspended with 500µL of Bambanker freezing medium (Cultek, cat. no. BB02). All this volume was then transferred into a cryovial and stored in a CoolCell (-1°C/min) inside a freezer at -80°C for 24h. After this period, the cryotube was moved to N<sub>2</sub> liquid tanks that belong to the Biobank of INCLIVA.

### **3.6 Thawing of cryopreserved organoids**

Frozen samples were introduced in a hot bath for a couple of seconds. This process was repeated approximately 2-3 times or until some liquid could be observed in the cryovial. At this point, the sample was partially thawed. Immediately, the contents of the cryovial were transferred to a 15 mL tube containing 5 mL of fresh BM. Then, the tube was centrifuged (1500 rpm, 5 minutes, 4°C) to separate the organoids from the DMSO. The supernatant was removed, and the pellet was seeded according to the protocol previously described in section 3.2.

### **3.7 Paraffin embedding and Hematoxylin & Eosin staining (H&E)**

Organoids of interest were fixed on their wells by addition of 4% formaldehyde. Fixation took place at 4°C and it lasted 45 minutes. Then, cold PBS was added to the wells and the droplets were broken manually. The contents were recovered and transferred to a 50 mL tube. The tube was centrifuged (500 xg, 10 minutes). Once it was finished, the supernatant was removed. After the centrifugation, an aliquot of histogel (Thermo Scientific, cat. no. HG-4000-012) was heated to 80°C using a thermoblock. The duration of this step was determined by the transition of the gel to a liquid state. Usually, it took 1 minute to obtain a liquid aliquot. Next, 5 droplets of melted histogel were transferred to the tube containing the fixed cells and resuspended with care. The tube was stored for a couple of minutes at -20°C. After this step, an histogel “brick” is extracted from the tube and transferred to a cassette. The cassette was given to the Pathology Department at HCUV. There, the cassette was introduced into an automated vacuum tissue processor (LEICA ASP6025), which dried and paraffin-embedded the sample. The processed block was left overnight at room temperature. The morning after, the block was cut into 5 µm sections using a microtome.

Before the Hematoxylin and Eosin staining, it was necessary to rehydrate the sections in order to remove the paraffin wax. This rehydration was performed by placing the sections in xylene (three washes – 5 minutes per wash), 100% ethanol, 95% ethanol, 70% ethanol and 50% ethanol (one minute wash) and lastly into distilled water (two washes - 5 min each) to complete rehydration. This last step was repeated twice. Lastly, the rehydrated sections were stained with Hematoxylin (Dako, cat. no. CS700) & Eosin (Dako, cat. no. CS701).

### **3.8 Immunohistochemistry**

The procedure followed for immunohistochemistry was very similar to the protocol described in the section 3.7 “Paraffin embedding and Hematoxylin & Eosin staining”. The same steps were performed up to the rehydration of the sample. Before antibody staining, there was a step of antigen unmasking using a 0.1 M citrate buffer, pH 6.0. The sections submerged in the buffer were introduced in an autoclave for a couple of minutes. After this procedure, the slides were washed with distilled water three times. Then, it was required to dampen/suppress the tissue endogenous peroxidase activity as it interfered with staining. Therefore, the slides were placed in Dako REAL™ Peroxidase-Blocking Solution (Dako, cat. no. S2023) for 10 minute and washed once using PBS. As a prevention of non-specific binding, a blocking solution, 2.5% horse serum (Vector, cat. no. S2012), was used for 20 minutes. Next, the samples were ready to be incubated with the primary antibodies. Prior to this step, the antibodies of interest were diluted using Dako diluent (Dako, cat. no. S0809). The samples and the diluted antibodies were incubated overnight at 4°C. The morning after, the antibody solution was removed, and the samples were washed thrice. Then, a solution containing the peroxidase-conjugated

secondary antibodies was added to each section and incubated for 45 minutes at room temperature. For the visualization samples were washed thrice again, followed by addition of Liquid DAB+ Substrate Chromogen System (Dako, cat. no. K3467). It was left for 10 minutes then briefly immersed in distilled water. Lastly, Hematoxylin was used to counterstain the sections, which stained the nuclei in a different color. Once all staining procedures were finished, the samples were first dehydrated (95% ethanol; 100% ethanol, xylene) then mounted with coverslips using Entellan (Merck, cat. no. 1.07961.0500) as the mounting medium. At this point, the sections could be visualized using an optical microscope. The following antibodies were used for immunohistochemistry: CK20 (Dako cat. No. IR777), Ki67 (Dako cat. no. IR626), MUC2 (Dako cat. No. IR658) and MUC5 (Dako cat. No. IR661). All antibodies were bought pre-diluted, format known as "Ready to use".

### 3.9 Immunofluorescence

Organoids of interest were passaged and grown in a P96W. Once they reached a good size and density, the organoids were fixed by addition of 4% formaldehyde. The fixation step took place at 4°C and it had a duration of 45 min. Then, cold PBS was added to the wells and the cells were recovered and stored in Eppendorf tubes. The next step was the permeabilization of the cells. The sample of interest was incubated with Triton 0.2% in cold PBS for approximately 5 minutes at room temperature.

Then, the content of the Eppendorf tube was centrifuged (500 xg, 5 minutes) and rinsed with PBS three times. Following this step, the cells were incubated with the diluted primary antibodies. Diluted antibodies proceeded from the combination of the primary antibodies for the markers of interest mixed in DAKO diluent (Dako, cat. no. S0809). This mixture containing the cells and the primary antibodies was incubated overnight at 4°C. Incubation took place under continuous low stirring. Next day, the content of the tube was washed three times with PBS and then, secondary antibodies were added to be incubated with the cells. This second incubation took place at room temperature and in the dark, lasting approximately 45 to 60 minutes. Lastly, the secondary antibody solution was removed, and the cells were rinsed thrice with PBS. After the washing step, the sample was mounted. The results were visualized using a confocal microscope (LeicaTCS SP8 spectral confocal microscope) located at the confocal microscopy unit at *Unidad Central de Investigación de Medicina (UCIM)* of the Faculty of Medicine at University of Valencia. DAPI was used for visualization of the nucleus along with antibodies for E-cadherin (Cell Signaling cat.no. 07/2012) and Ki-67 (Dako cat. no. IR626). E-cadherin was used in a 1/200 dilution; Ki-67 was a "Ready to use" antibody.

### 3.10 Genomic DNA extraction

DNA extraction was performed using two different sources: tumoral tissue and the corresponding tissue-derived organoids from the same patient.

- **Tissue DNA extraction**

The AllPrep® DNA/RNA Mini Kit (Qiagen, cat. no. 80204) was used. The first step was to weigh the available tissue and collect 20-30 mg for the extraction. Once it was weighed, tissue was disrupted and homogenized using the TissueLyser system (Quiagen), a process that took 10 minutes. Disruption occurred by agitation in presence of a stainless magnetic bead (Qiagen, cat. no. 69989) and RLT buffer (provided in the kit). Then, the homogenized lysate was transferred to an AllPrep DNA spin column. The rest of the steps required for extraction were performed following the instructions found in the kit's protocol.

- **Organoid DNA extraction**

The organoids required a different kit for the extraction of the DNA. This kit was QIAamp® DNA Micro Kit (Qiagen, cat. no. 56304). Organoids were taken from one well, in which high organoid density was observed. In order to retrieve the organoids, the droplet was broken down with cold PBS and the content of the well was transferred to a tube. A lysis solution that contained a Proteinase K buffer was added to the tube and the mixture was incubated for 4 hours in a thermomixer at 56°C. After this incubation, 200 µL of AL buffer was added, and the tube was briefly vortexed. Then, 200 µL of ethanol were added, thoroughly mixed, and incubated for 5 minutes at room temperature. After these steps, the final lysate was obtained and transferred to a QIAamp MinElute column. The rest of the steps required for extraction were performed following the instructions found in the kit's protocol.

Nuclease-free water was used for DNA elution. For DNA quantification, absorbance was measured using Nanodrop (1 µL).

### **3.11 Genetic sequencing using a customized panel**

DNA extracted from both tissue and organoids was sequenced using a customized panel containing 85 genes. This panel contained most of the genes involved in CRC development and progression. APC, that presents a mutation in 90% of the CRC cases, KRAS, NRAS and PI3KCA among others were present in this panel.

The design of the panel, sequencing and raw data analysis was carried out by the Precision Medicine Unit from INCLIVA.

### **3.12 Drug assay**

Droplets from 2 wells containing organoids of interest were recovered by breaking the droplet manually using cold PBS, introduced into a 50 mL and centrifuged (1500 rpm, 5 min, 4°C). The organoid sediment was digested to single cells by adding 200µl of trypsin for 5 minutes at 37°C. Cells were observed in the microscope to assess how digestion was progressing. Once cells were completely disaggregated, BM was added to the tube to inactivate the trypsin. Then, cells were counted to determine the number of droplets that could be generated taking into account the following parameters: each well contained a 5 µL-droplet and cell density was established as 5.000 cells per well in a p96w plate. After the estimation, it was possible to assess the effects of 5-FU individually (Condition 1), Oxaliplatin individually (Condition 2) and as a combination (Condition 3). Eight concentrations (0.1, 1, 5, 10, 50, 100, 150, 200 µM) of each condition were analyzed in triplicates (Schematic distribution can be found at **Appendix – Supplementary figure 1**). Drugs were provided by the Pharmacy Service at HCUV. The generation of the droplet and seeding followed the steps from section 3.2.

Organoids were left to grow for approximately 48h. After this period, they had grown well, so the culture medium was aspirated and treatment (drug + medium) was added. The plates were incubated 5 days at 37°C and 5% CO<sub>2</sub>. For this assay, the control wells contained PBS, the vehicle in which the drugs were diluted.

After the exposure period finished, CellTiter-Glo® Luminescent Cell Viability Assay (Promega, Cat. #G7570) was used for the quantification of the effect of drug treatments on the organoids' viability following manufacturer's instructions. Briefly, 500 µL of CellTiter-Glo reagent was added in each well, the content was mixed, and the plate was incubated for approximately 10 minutes. CellTiter-Glo is an assay that detects viable cells based on the amount of ATP present in living cells. This assay allows for a homogeneous visualization, in which the only step is the addition of a single reagent, a luciferase. Lastly, luminescence was measured using a luminometer.

## **4. RESULTS AND DISCUSSION**

### **4.1 OBJECTIVE 1: Fine-tuning the protocol for the generation and growth of the organoids by finding the most suitable percentage of Matrigel**

Prior the elaboration of the protocol used in the generation of organoids several parameters had to be established. Different tests were carried out to determine the most suitable conditions for the generation of the organoids. Objective 1 was focused on how organoid growth was affected by the Matrigel used in the elaboration of the 3D droplet. Matrigel can mimic the *in vivo* environment. It is a mixture of Extracellular matrix (ECM) proteins such as laminin, collagen IV and entactin. These proteins are obtained from Engelbrecht-Holm-Swarm tumors in mice (Kleinman & Martin, 2005).

Two wells from CTO65-P02 (tumoral organoids) were used. Data for the analysis of several parameters such as growth rate, generation and morphological changes was obtained. In order to obtain reliable results and gain a better understanding of the generation and evolution of the cultured organoids, markings were made in the plate to ensure that pictures taken for monitoring belonged to the same area. The assessment lasted 6 days. During the assay, the organoids were not passaged but medium was changed. It was observed that this specific line grew fast.

#### **4.1.1 Growth rate and generation rate**

The starting point for this procedure was the recovery of organoids cultured under the conditions mentioned in Materials & Methods. Following the protocol described in section 3.4, the droplets containing the organoids were broken down and recovered in a tube. Then the cells were trypsinized and re-seeded with different Matrigel concentrations in a P96W (Volume of the droplet: 5  $\mu$ L). Each well contained a cell density of 1000 cells/ $\mu$ L. 8 concentrations of Matrigel were assayed: 5, 10, 15, 20, 25, 50, 75 and 100%. **Appendix - Supplementary figure 2** shows selective images of the monitoring at day 1, and day 6 of culture.

To quantify the growth differences observed under the microscope, images were processed using IMAGEJ. The area of 10 organoids per assayed condition was measured across different days of culture. According to **Figure 7**, we can assume that in general lines a higher growth rate was observed at medium/low concentrations, being 50% the most optimal concentration, as it was the one in which the highest mean area was observed. This condition was followed by the lower range of concentrations (<50%) and the worst growth was observed at high concentrations (>50%), being 75% and 100% the worst.

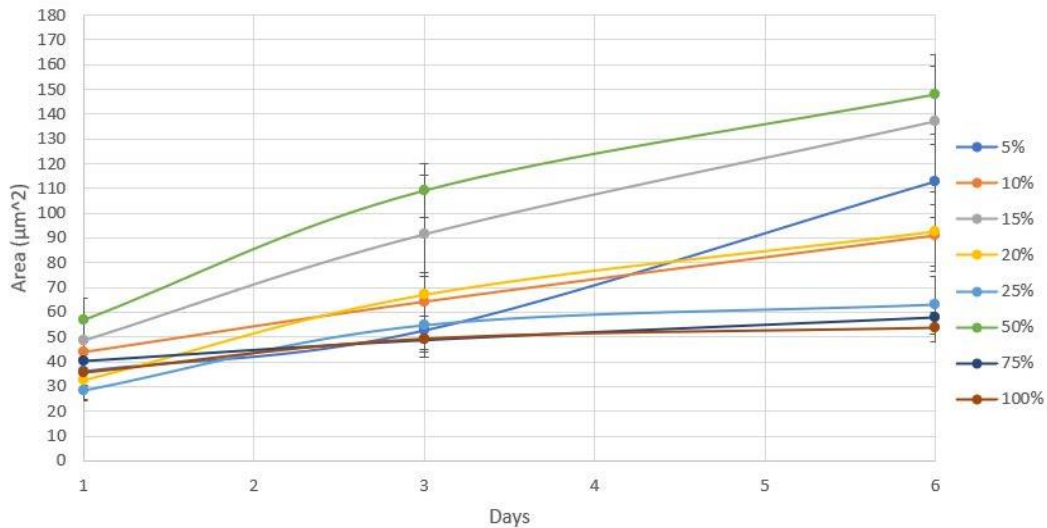


**Figure 7. Growth of organoids cultured in different Matrigel concentrations.** Each color corresponded to a different condition (graph legend on the right). Growth was determined measuring the mean area of 10 organoids (at 5X magnification) using ImageJ. For day 1, any structure made of more than one cell was considered as an organoid; for day 6, small structures were not considered as organoids. Y axis: Area ( $\mu\text{m}^2$ ). X axis: Days in culture. Measurements represented in the graph: mean area  $\pm$  standard deviation.

High Matrigel concentrations yield the smallest organoids and the lower growth rate, so it was not suitable for our experimental procedure. We can hypothesize that higher concentrations did not allow for the organoids to grow bigger as Matrigel constitutes a very dense matrix that traps them in a specific position and leaves no room for growth. Some authors have argued that at those concentrations, Matrigel is very viscous and generation of the droplet is very difficult as it gels fast (Ahmad *et al.*, 2014). Concurrently, lower concentrations allowed for obtention of organoids with high mean area, reaching high values similar to 50% in the case of 15%, but lower concentrations were also precarious as very diluted Matrigel creates a more fragile gel, which hindered culture maintenance. Integrating all these parameters, the most suitable concentration to obtain an optimal growth was 50%, hence we used it for the generation of the organoids in the protocol.

The same experiments were used to evaluate the influence that the percentage of Matrigel had on organoid generation. It was possible to calculate this parameter because the same cell density was seeded for all conditions. The number of organoids present at day 6 was used to estimate the generation rate. In this evaluation, we considered three main Matrigel concentrations (Low, Medium and High). For low Matrigel concentration (concentrations under 50%), an average of  $44 \pm 8$  organoids was obtained. In 50% Matrigel concentration, an average of  $> 100$  organoids was observed and in high Matrigel concentrations (concentrations above 50%), an average of  $20 \pm 3$  was observed. The highest generation rate was observed at 50% Matrigel, giving more support to using this concentration when generating colon tumoral organoids.

#### 4.1.2 Morphological evolution

Once it was determined that the different Matrigel concentrations affected the organoids growth, we studied whether morphology of the generated organoids was affected also by the diverse culture conditions. The analysis was performed by examination of the organoids generated in the section above 4.1.1. Comparison between two days of measurements, day 3 and day 6, were established in order to compare the changes as culture time progressed (**Figure 8**).

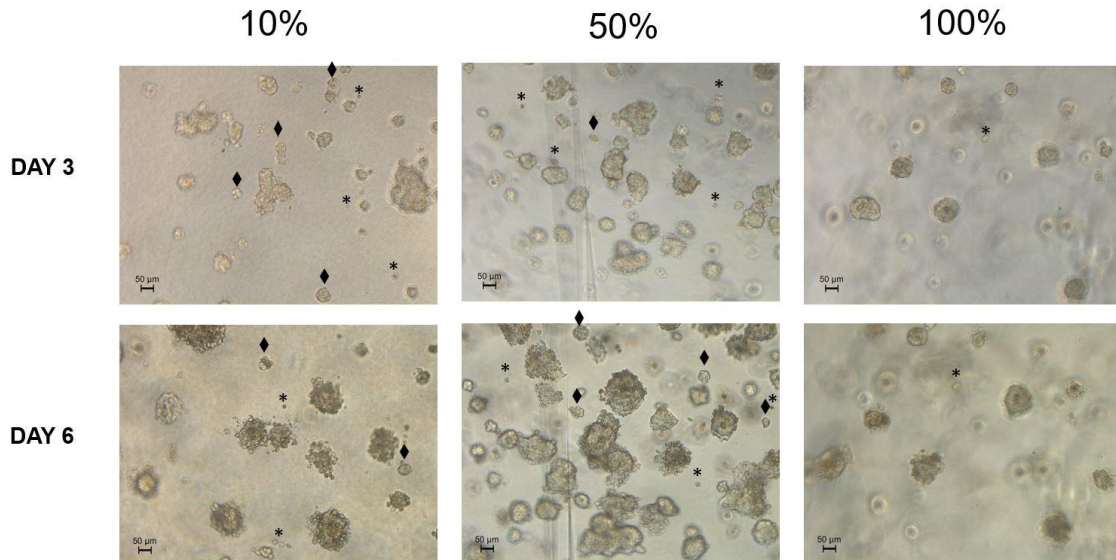


**Figure 8. Evaluation of organoid morphology in different culture conditions (Low, High and Medium Matrigel concentration).** Images correspond to organoids at 10x magnification from day 3 and day 6 at 10%, 50% and 100% Matrigel concentration. Scale bar: 50  $\mu$ m. Some examples of different morphology were highlighted: large structures with central lumen (unmarked), single cells (asterisks), clusters of small cells (diamond).

As other author previously described (Fujii *et al.*, 2018) different morphologies could be also identified in our organoids culture: single cells, clusters of several small cells, larger structures in which a central lumen could be identified...

From these pictures, it could be determined that the range corresponding to Low Matrigel (<50%) concentration showed organoids with diffuse borders, being very difficult to keep them in focus with the microscope. Big structures were not uniform and seemed to be made of several smaller spheres lumped together. Some adherences were found, and organoids were very dark. On the other hand, high Matrigel concentrations (>50%) allowed the formation of solid organoids with no buddings, probably due to the increased stiffness of the matrix (Broguiere *et al.*, 2018). The 50% concentration showed spherical structures that are more defined. Organoids are rounder and look more uniform. Borders of each organoid can be clearly traced. Cystic organoids, which are characteristic of their tumoral origin, can be identified.

Further analysis to confirm these characteristics in a more objective way could be conducted using H&E staining, however due to COVID-19 pandemic we were not able to study it.

Overall, within the range of 50% Matrigel we obtain the highest growth, along with a well-defined morphology. The generation rate is also the highest at this concentration. For all of these reasons, 50% Matrigel was the concentration used in the established protocol for the generation and maintenance of organoids as it offered the most suitable

stiffness and the most adequate density as an ECM, maximizing organoid growth. These findings were further confirmed by previous researchers such as Ahmad et al. (2014).

## **4.2 OBJECTIVE 2: Generation and maintenance of organoids derived from: colonic tumoral and non-tumoral tissue, liver metastatic tumoral tissue and rectum tumor tissue**

During the elaboration of this thesis, 5 different organoid lines from tissue samples were generated. It is possible to classify the organoids in three major groups, depending on their origin:

### **4.2.1 Colon tumor and peritumoral organoids**

Tissue samples from patients undergoing tumor removal were collected in order to generate organoids. Among these samples, tumoral and peritumoral tissue were taken from the same patient, allowing for future comparisons between normal and tumoral tissue. Due to the size of the tumoral specimen, it was possible to sample from two different regions within each tumor, designated as P01 and P02. Two lines were generated: CTO65-P01 / CTO65-P02.

Differential sampling is very important for research as tumors are highly heterogeneous, hence it allows for a more comprehensive analysis of the tumor nature and molecular mechanisms. Along with the tumoral samples, surrounding non-tumoral tissue was taken and organoids were generated, denoted as CNO65. Generation of normal organoids may allow for comparisons and genetic screenings with the corresponding tumoral samples.

These organoid lines were generated, passaged, and maintained following the protocols described in section 3 "Materials & Methods". The droplets containing the organoids were constituted by 50% Matrigel, as it was the most optimal concentration according to our fine-tuning (see Objective 1). CM was used with the tumoral samples, while the normal samples were cultured with ST medium. CM's composition was specifically designed by our research group and its detailed composition can be found at Materials & Methods. It contains all the known growth factors that favor tumor growth in concentrations carefully adjusted. The objective was to mimic the conditions present at the stem cell niches within colonic crypts. It also lacks factors that could promote normal growth over tumoral growth such as Wnt3A. More than 90% of colon tumoral cells have mutations that constitutively activate the WNT pathway whereas normal cells require Wnt3A for growth. Thus, the absence of this factor in tumor organoid culture prevents the outgrowth of normal organoids.

ST was a commercially available medium, of unknown composition, but specifically designed for intestinal normal organoid growth. The medium was supplemented with antibiotics to prevent bacterial growth. Detailed composition of this medium was described in Materials & Methods.

In general, collected samples did not have a uniform size, but in both cases samples from non-tumor adjacent tissue were approximately 4x4 cm, whereas tumoral samples were smaller. Non-tumoral tissue was more difficult to process because it contained a lot of mucus. The number of cells obtained was quite low for both lines. Consequently, only three wells were used per patient: one well for the nontumoral organoids, one well for the tumoral organoids P01 and one well for the tumoral organoids P02. Organoids

from P02 grew well so in the next passages it was possible to generate 2-3 wells per broken droplet.

As an example, in **Figure 9** we can observe the CTO65-P02 organoids, which showed the main features described in literature: central lumen surrounded by polarized epithelium. Organoids were cultured and passaged several times, so a continuous reserve for future studies could be ensured.

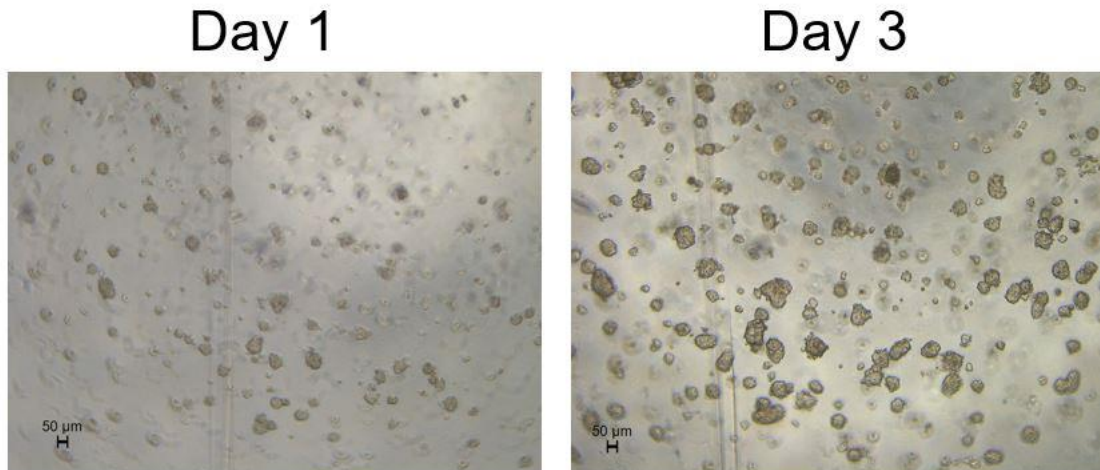


**Figure 9. Generation and maintenance of CTO65-P02 (localized colon tumor organoids).** Organoids at passage 4, day 1 (Left). Organoids at passage 4, day 3 (Right). Images taken at 5X magnification.

#### **4.2.2 Metastatic colon organoid**

Generation of metastatic organoids, and their maintenance, followed the same protocols established in Section 3 “Material & Methods”. mCTO50 line was established. In this case, the metastatic spread had reached the liver. A small biopsy was used as the starting material for the generation and CM was chosen as the medium for metastatic organoid culture as the composition favored the growth the most. Despite the small size of the sample, 2 wells were established. Evolution of the generated line can be observed in **Figure 10**.

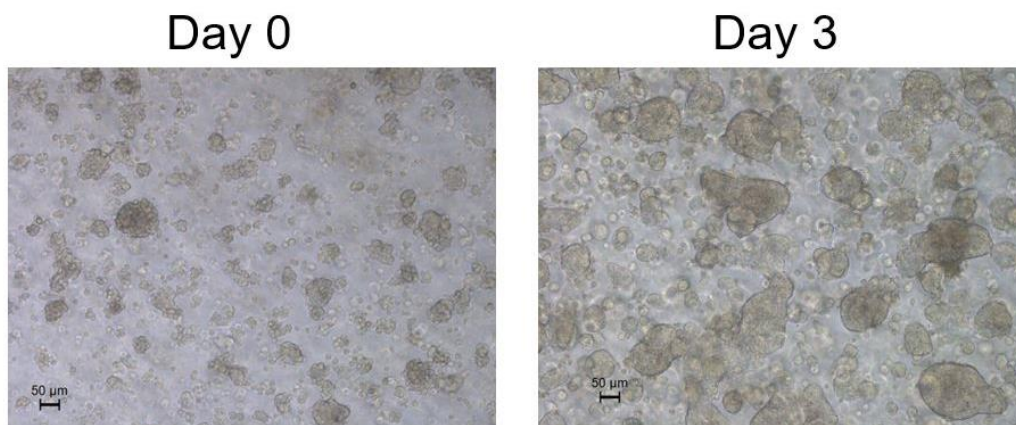


**Figure 10. Generation and maintenance of mCTO50 (metastatic colon organoids).** Organoids at passage 8, day 0 [hours after seeding] (Left). Organoids at passage 8 day 3 (Right) mages taken at 10X magnification.

These images showed an organoid line with fast growth and very high density. Pictures were taken on day 0 and it showed bigger organoids (compared to localized tumoral organoids) and lots of small single cell structures, which had the potential to give rise to new organoids. Big lumens were characteristic of this line.

Interestingly, it had been later confirmed that the patient had a hypermethylation of the MLH1's promotor, which leads to MSI. MLH1 is a mismatch repair gene, thus it encodes for a protein involved in DNA repair. This mutation has been associated with Lynch's syndrome, a hereditary non-polyposis colon cancer.

#### **4.2.3 Rectum organoids**

Two lines of rectum organoid were established: RTO8 and RTO10. The protocol used for the generation and maintenance rectum organoids was described in section 3. "Material & Methods". Sample size was not measurable as it consisted of several fragments. It was possible to establish 2 wells. The culture medium used with these organoids was STA medium (composition of the medium described in Materials & Methods). The choice of the medium for this type of cultures was based on previous studies carried out by the researchers at the laboratory where I collaborated. They performed several assays comparing different culture media in order to determine which medium works best for each type of sample.

Rectum organoids were not as easily established as other types of organoids (**Figure 11**). At day 1, we observe that most of the structures are single cells and several big dark complexes. There was lot of debris in both wells. Unfortunately, the evolution of this specific line was not possible as at day2 of culture, contamination on the wells was detected and the organoids had to be discarded.

Day 1

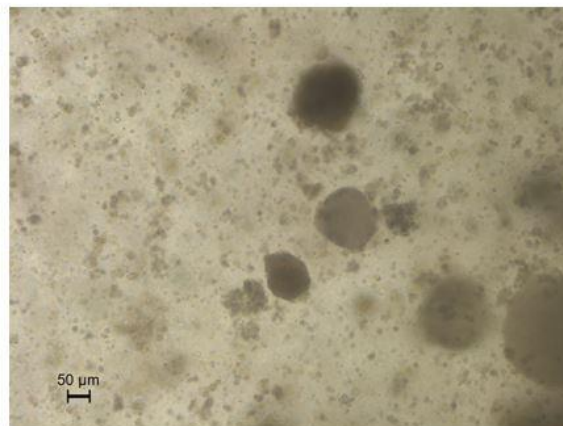


**Figure 11. Generation and maintenance of RTO8 (rectum organoids).** Organoids at passage 0, day 1. Image taken at 10X magnification.

### 4.3 OBJECTIVE 3: Morphological and molecular characterization of the organoids

Ideally, the characterization of all the organoids generated in the previous section should have taken place. However, due to COVID-19, further characterization for some of them had to be stopped. Most of the procedures regarding morphological analysis were performed with organoids previously established in the laboratory, whereas it was possible to use localized tumor organoids generated in the previous section for part of the molecular characterization. These analyses were performed to validate that patient's derived organoids were a reliable model of the disease because they mimicked the biological characteristics of the primary tumors.

#### 4.3.1 Morphological analysis

Organoids generated in the previous section did not reach the densities required to perform these assays with one exception: mCTO50. This metastatic line grew very fast and the organoids were big, so they were studied via Hematoxylin & Eosin staining.

##### 4.3.1.1 Hematoxylin & Eosin staining

H&E staining was used to analyze the structure of the organoids. Hematoxylin stained the nucleus blue whereas eosin was used as a counterstain, which colored the cytoplasm in pink (**Figure 12**). It showed that the organoids were constituted by a monolayer of polarized epithelial cells surrounding a central lumen as it can be seen in the CTO36. On the other hand, metastatic organoids presented more compact structures with different lumens, as mCTO50 showed organoids without it or with very small lumens whereas mCTO47 showed thin "elongated" lumens. This figure exemplified that despite having the same origin (colon metastasis found in the liver), each patient's organoids had different characteristics. H&E showed that we were working with tumoral cells but further characterization using Immunohistochemistry and Immunofluorescence would be required to know more characteristics of the tumor, such as confirmation of its intestinal origin or if it had high proliferation.

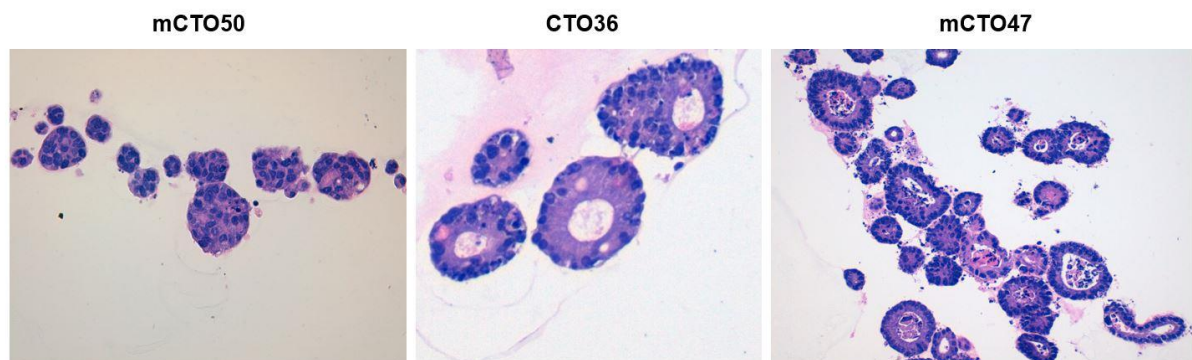


**Figure 12.** H&E staining of tumoral and metastatic organoids. Images taken at 40X magnification (mCTO50) and 20X magnification (mCTO47 & CTO36).

##### 4.3.1.2 Immunohistochemistry

Immunohistochemistry was used for the characterization of rectum organoids. Markers that have been associated to progenitor cancer cells were assessed, including Ki67, CK20, MUC2 and MUC5 (**Figure 13**). Ki67 is a marker linked to a proliferative status. CK20 is a cytokeratin, found in the cell membrane. It has been regarded as a

marker for progression of CRC cancer and it has been associated with the structural integrity of the cells. Lastly, two mucins were studied. MUC2 and MUC5 are gel-secreting mucins, usually located in the large bowel mucosa and gastric epithelium, respectively. It has been established that both mucins have opposite expression patterns. Both have cytoplasmic pattern. Muc2 has been associated with tumors of colonic origin (mucinous types) whereas MUC5 expression has not been associated to CRC carcinoma.

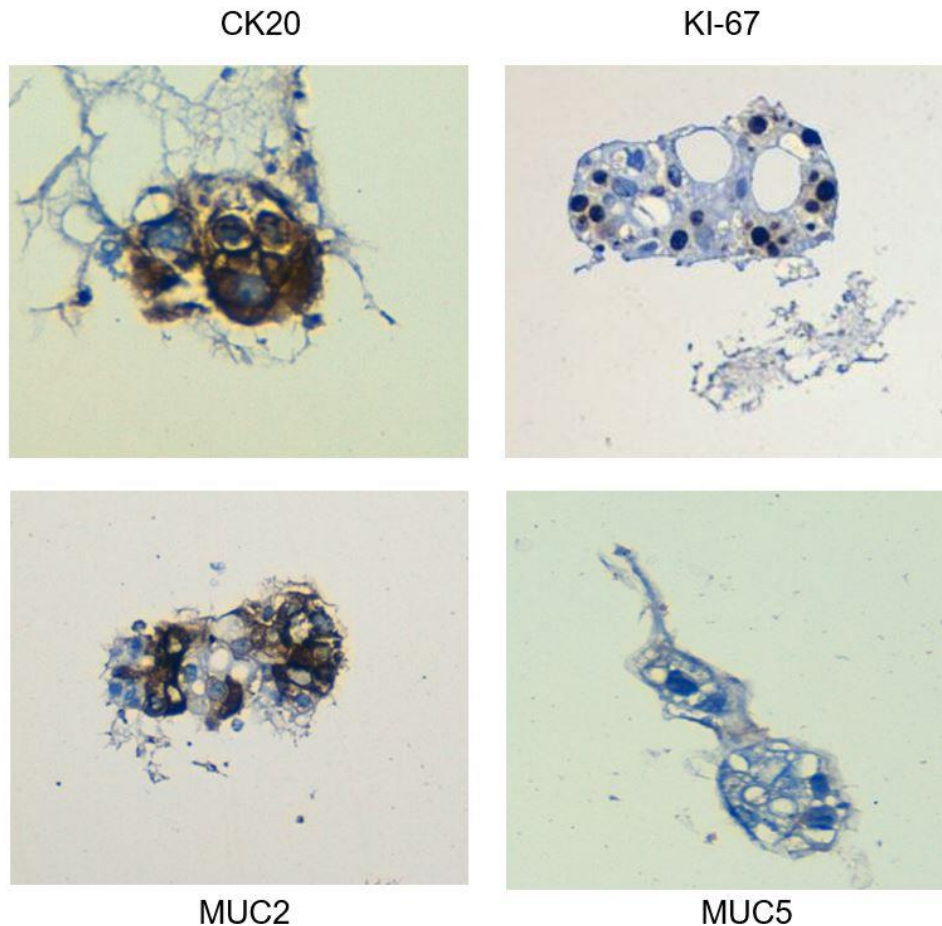


**Figure 13. Immunostaining of rectum organoids.** CK20, Ki67, MUC2, MUC5 were analyzed. Images taken at 40X magnification.

CK20 signal is dispersed across the organoids structure, marking the cell membranes. KI-67 expression is located within cell nucleus and it indicated that cells constituting the organoid retained their proliferative activity. Cancer cells are continuously growing, thus positive Ki67 staining in the nucleus was expected. Both markers allowed us to determine that colon tumoral cells are part of the structure.

The expression of the mucins was opposite, which was expected. Literature was examined to analyze the effects of said pattern of expression. Previous studies have correlated worse survival of the patient with the loss of MUC2, hence its importance. High MUC2 levels have been commonly associated to higher cell differentiation and lower probability of developing metastasis in the lymph nodes (Wang *et al.*, 2017). On the other hand, the absence of MUC5 staining has been used as a prognostic factor for aggressive CRC carcinoma (Kocer, 2002). Authors such as Perez *et al.*, 2008 considered that absence of MUC5 could lead to worse prognosis in mucinous rectal cancer.

#### 4.3.1.3 Immunofluorescence

Immunofluorescence was performed on Colon Adenoma Organoids (CAO). E-cadherine, DAPI and Ki67 were the selected markers for assessment. Firstly, E-cadherine (E-cad) is defined as a cell-cell adhesion molecule, hence located on the cell membrane. It is a marker usually absent in cancer cells that undergo Epithelial-Mesenchymal Transition. DAPI is a fluorescent marker that binds strongly to A/T DNA regions; hence it stains the nucleus. Ki-67 was used to determine the tumor proliferative activity; the nuclear expression is assessed (**Figure 14**).

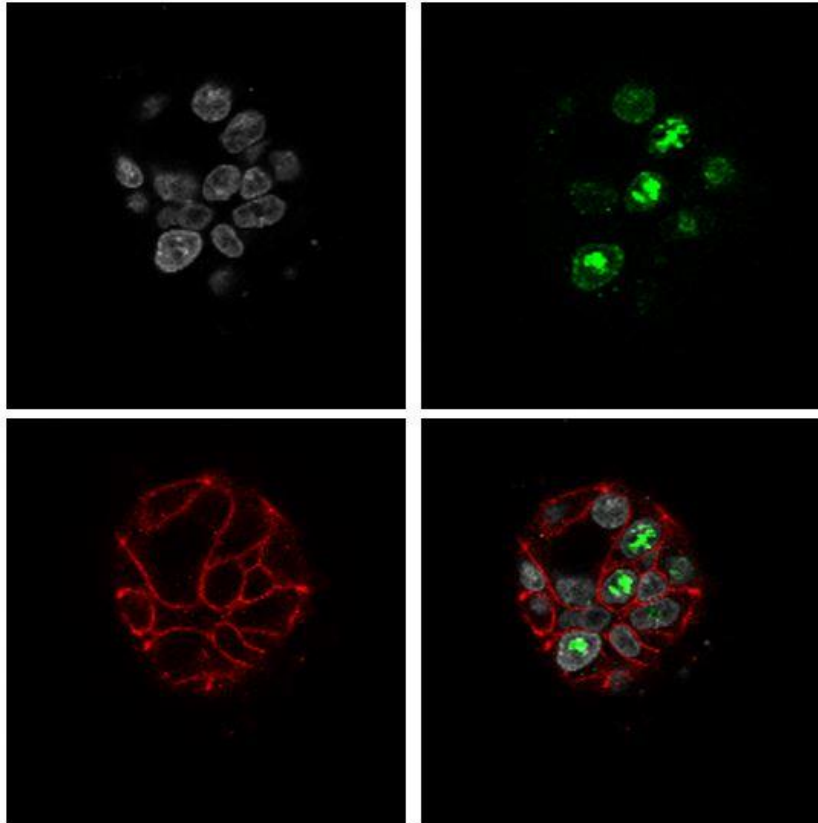


**Figure 14. Immunofluorescence of adenoma-derived organoids (CAO29).** Confocal microscopy was required for visualization. E-cad: Red, Dapi: Grey, Ki67: green. Both individual pictures for each marker and the merge of all were analyzed. Images taken at 40X magnification.

These pictures showed that an organoid is a structure constituted by individual cells that assemble to form the 3D complex. DAPI was used to stain the cells' nucleus revealing that they self-organize. The level of Ki67 was high and located in the nucleus, which was expected as they are proliferating. DAPI also confirmed that Ki-67 is localized within the nucleus. It is known that E-cad is involved in cell interaction and located within the cellular membrane, and this statement was confirmed in the third picture – red signal –, in which we determined the borders of the cells. All markers together showed that an organoid is constituted by individual cells that assemble and that some of them retained their proliferative activity. Our observations matched with the characterization carried out in previous studies and literature (Nussrat *et al.*, 2011; Fujii *et al.*, 2018).

### **4.3.2 Molecular characterization by Next Generation Sequencing using a customized panel**

An organoid must retain the main characteristics of the tissue of origin to be used as a reliable preclinical model. Nevertheless, sequencing also had a secondary objective. As organoids are constituted from aSCs derived from the tissue of origin, it was possible to generate a wide variety of different clones. It is not an overstatement to say that at this point, sequencing of organoids could also be used to register mutations in very low frequencies that may have remained masked when sequencing the whole tissue.

These mutations can have a key role in understanding how the disease had evolved or how it had spread, and it could be used to design a personalized treatment that grants a successful recovery.

Both tissue (CTT65) and tissue-derived organoids (CTO65) generated from the same patient were used for the molecular characterization. DNA was extracted following the steps described in Materials & Methods. Prior to sequencing, quantification of the DNA and assessment of its quality was carried out using Nanodrop. Acceptable values were obtained so the DNA samples were given to the Precision Medicine Unit. Sequencing took place using a customized panel with 85 genes that had been correlated with CRC. The Precision Medicine Unit from Incliva executed design of the panel, sequencing and raw data analysis. The results were summed up in **Table 1**.

**Table 1. Mutation frequency of CRC-related genes comparing CTT65 (tissue) and CTO65 (tumor organoids).** Sequencing data was filtered, removing those mutations that caused synonymous variants, keeping mutations with a frequency above 5% and at least 100 reads. The table does not contain every gene sequenced, only those alterations present both in tissue and organoid or that were fulfilled the mentioned filtering criteria. Percentages were calculated based on the number of individual reads per gene over the total number of reads performed. Highlighted gene indicated that said mutation could have a high impact. HGVS Human Genome Variation Society protein sequence name.

Gene	Mutation	HGVS <sup>p</sup>	Frequency in Organoid(%)	Frequency in Tissue (%)
KRAS	Missense	p.G12D	64	20,89
BRCA2	Missense	p.A3205P	30,24	40
BRCA2	Missense	p.A3205V	30,5	39,81
TP53	Missense	p.R273H	100	14,71
BRCA1	Missense	p.P871L	52,94	52,87
ALK	Missense	p.R1214C	52,23	15,18
PIK3CA	Missense	p.E545K	53,63	9,52
APC	Nonsense	p.R283*	24,58	11,84

Observing the data in the table, organoids present the same mutations as the ones found in the tissue, hence we confirm that they are a reliable model of the disease found in the patient. Genes with clinical relevance are further analyzed, including KRAS, BRCA2, TP53, APC, PIK3CA, ALK... Missense mutations were predominantly observed for most of the studied genes. Taking KRAS as an example, missense mutations are common, and some authors even considered it a hallmark. In our samples, KRAS mutation was at codon 12. Previous studies, showed that KRAS mutations affected different residues, including G12, leading to the synthesis of a mutated protein that is always activated, promoting cell proliferation (Kamburov *et al.*, 2015). The presence or absence of such mutations is essential when choosing a treatment because these mutations can confer resistance to treatments. For example, anti-EGFR therapies do not work with patients carrying a mutation in KRAS (Benvenuti *et al.*, 2007), hence it would not be a suitable treatment.

Another interesting mutation was organoids' BRCA1 mutation that account for 50% of the reads, in the available literature there is controversy surrounding the role of this mutation on CRC. Another relevant gene is APC, which is a negative regulator of Wnt signaling pathway, in charge of cell proliferation and differentiation. Inactivation of APC gene occurs in more than 80% of the cases of sporadic CRC and leads to uncontrolled  $\beta$ -catenin activity and continuous activation of the Wnt pathway (Kwong & Dove, 2009).

Lastly, TP53 encodes for a tumor suppressor protein involved in cell cycle arrest, regulation of apoptosis, senescence, and many other cellular processes. Missense mutations within TP53 are very common, especially within the DNA binding domain (R273 is considered a hotspot) and it led to a gain-of-function, favoring the oncogenic progression. Moreover, previous findings have demonstrated that additionally to the mutation, there is a loss of the remaining wild-type allele caused by a phenomenon known as loss of heterozygosity (LOH). These circumstances have been linked with poorer survival, an increase in the proliferation of cancer stem cells and an accelerated malignant progression (Nakayama & Oshima, 2019)

Our findings showed that TP53's R273H mutation had a frequency of 100% in organoids, which means that organoids display both the mutation and the loss of the remaining wild-type allele by loss of heterozygosity. However, when examining the tissue, we could not find such high frequency. Frequency values were lower than 50%, hence, an indication that not all the cells within the tumor had the TP53 mutation or the loss of heterozygosity. A possible explanation for this situation is that we could consider it as an indicator of intratumoral heterogeneity. We had taken samples from one region that showed high mutation frequency, but it was not extrapolated to the tumor, hence targeting that mutation may not be the most effective treatment. It has to be said that bias towards the mutated TP53 could also have been introduced during culture as a positive selection of LOH TP53 organoids could happen.

This illustrated the importance of multi-regional sampling, if possible, as considering tumor heterogeneity is crucial in the application more efficient therapies that suit each patient.

Overall, we also observed that mutations were more abundant in organoids compared to the tissue of origin. This may seem unusual, but it can be explained as follows: organoids represented "pure" tumor DNA, as they were constituted by tumoral epithelial cells carrying the mutations, whereas within the tissue sample, several cell types could be found. Besides tumor cells, fibroblasts, macrophages, endothelial cells, immune system cells such as lymphocytes and other cells commonly found within the tumor microenvironment were present. Tumor-associated mutations were diluted when analyzing such number of different cells, leading to lower mutation frequency within the tissue. Analysis of the organoids allowed the detection of this low frequency mutations with higher sensitivity as only tumor cells are sequenced, hence why the values were higher for most of the studied genes.

In conclusion, we have managed to prove that organoids do imitate the traits of the tissue of origin and they are suitable preclinical models for CRC's studies. Organoids are a new model system with great potential, especially for the personalization of treatments, so that therapies are designed taking into consideration each patient, individually. The ability of replicating the *in vivo* response with high accuracy offers researchers the possibility for drug screening and drug development.

#### 4.4 OBJECTIVE 4: Determination of the sensitivity of the generated organoids to current treatments

Among the applications of organoids as a preclinical model for cancer research one of the most frequent application is the drug sensibility assay. Results provided by this assay will give information about dosage and response to the treatment in the organoids, information that could be extrapolated to the patient's state and help oncologists to take decisions on the most suitable treatment for the patient.

However, results cannot be translated to the clinic as easily as it sounds. Firstly, organoids have to be tested to prove that the response towards the treatment is identical to the response observed in the patient. This analysis is performed via optimization of the drug assay to the characteristics of the patient of interest. In our case, CTO65-P02 organoids were chosen for the drug assay. These organoids were characterized from a molecular point of view – via sequencing - in the previous section, showing that they are suitable models as they imitate most of the tumoral characteristics and an acceptable correlation between tissue and organoids was found.

The treatments chosen for this assay were drugs that were administered to the patient too, in order to see if the response observed in the organoids was the same as the one observed in the patient. Two different therapies were studied: 5-FU and Oxaliplatin. 5-FU is a chemotherapy drug whose action relies on stopping the uncontrolled cell division, a characteristic of tumoral cells. It has been defined as an antimetabolite drug that is taken by the cells using the same mechanisms as normal metabolites and halts division in a cell-cycle specific way. 5-FU is a pyrimidine analogue, more specifically an uracil analogue. Its mechanism of action can be summed up as the inhibition of the thymidylate synthase activity required for DNA synthesis and its metabolites can hinder RNA processing. On the other hand, Oxaliplatin is a platinum derivative. It is designated as chemotherapy drug mainly used in metastasized colon patients and its action is directed towards actively dividing cells. However, oxaliplatin is classified as an alkylating agent, which works in a cell-cycle nonspecific manner, being more active on cells that are in the interphase.

As mentioned above, organoids from CTO65-P02 were used for this assay. Prior to its use, they were passaged and left to grow for a couple of days. The passaging, duration of the treatment and the instructions for the visualization of the effects can be found at Materials & Methods, section 3.12. Three different conditions were assayed: only 5-FU, only Oxaliplatin and combination of 5-FU and Oxaliplatin. For each condition, seven different concentrations were assayed (0,1; 1; 5; 10; 50; 100; 150; 200  $\mu$ M) and PBS was used as positive control, as it was the vehicle in which drugs were diluted. Blank wells were used as negative control. Three replicates for each assayed compound were used.

The effects of the treatments were evaluated as the effects that they had on organoids' viability, measured using CellTiter-Glo. In the analysis of the results, we established the average value for each condition, including an average from the blank wells and from the control wells. Then, the average of the blank wells was subtracted from all the rest of the values, and the average from the control wells was determined to represent 100% viability as it was the positive control. The rest of the viability values were calculated taking into account the control wells (**Figure 15**).

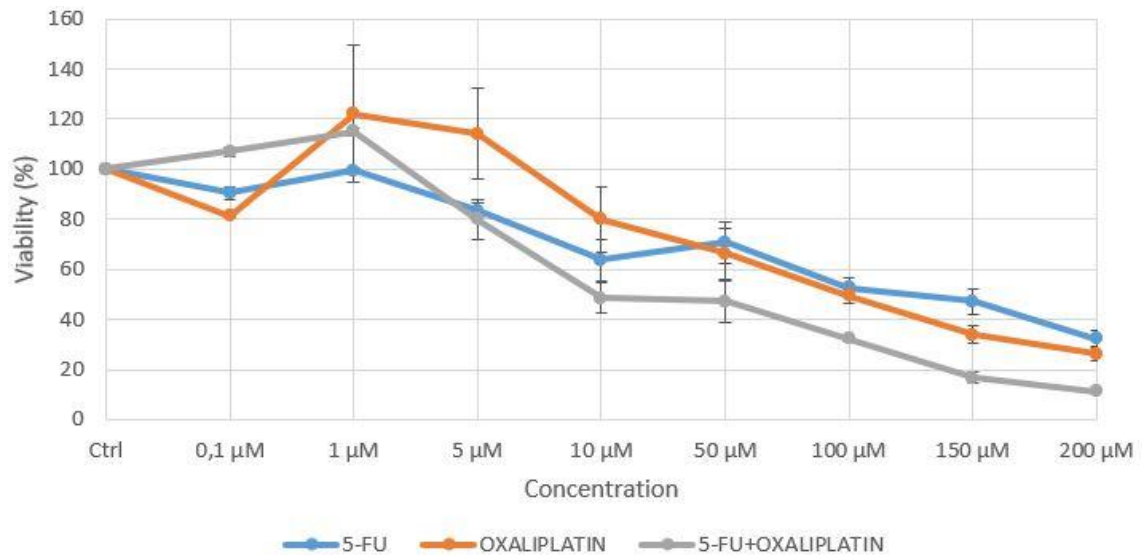


**Figure 15. Comparison of the effects of each monotherapy and the combined therapy on CTO65-P02 organoid viability.** Figure with all the assayed conditions in the same graph. Treatment lasted for 5 days. The effects of these drugs were visualized using CellTiter-Glo. Viability was calculated as the average of the replicates taking into account that the control represented 100% viability. Before the estimation of the average viability values, all wells were normalized using the values from the blank wells. Average viability  $\pm$  standard deviation was represented in this graph.

It should be mentioned that during the seeding of the organoids some problems were encountered, specifically regarding the first replicate for lower concentrations. These outliers were removed from further analysis, but it may have affected the results and measurements hence the disparity in the obtained viability. Due to COVID-19, the assay could not be repeated.

Overall, we observed that higher concentrations had a greater impact on organoids survival and that viability tended to decrease in a dose-dependent manner. Administration of the combination of drugs showed better results than administering each drug independently, thus it could be considered as the more efficient treatment. This statement is supported by **Figure 15**, in which we observed that viability decreased under 50% with a lower concentration compared to “only 5-FU” and “only Oxaliplatin”.

Focusing on each individual treatment, we observed that there is also a dose-dependent viability reduction, except for lower concentrations – mainly below 5  $\mu$ M -. These conditions in which we could find anomalies were affected by complications during seeding procedure which may have caused the disparities detected.

In conclusion, there is a need to improve the seeding procedure, and the execution of the assay as the results obtained cannot be considered completely adequate. For example, in some concentrations of the treatment, the organoid's viability values are above the control. However, this assay showed that the combined therapy was better than the monotherapies. Variability at lower concentrations for 5-FU and Oxaliplatin were deviations from the expected pattern but it only influenced the lower range. Ideally, this drug assay should be repeated making two independent experiments (experimental duplicates), modifying the seeding procedure to suit the characteristics of the assay, and using triplicates for each condition. This way more data would be generated and compared.

All in all, organoids allowed for an in-depth study for the effectiveness of different treatments and their combination, showing which therapy is more suitable for each patient, and once again leading to a personalized approach to cancer treatment.

## **5. CONCLUDING REMARKS**

In this thesis:

-The techniques for the generation and maintenance of organoids were fine-tuned to improve their potential. Growth rate, morphological evolution, and generation rate were assessed comparing different Matrigel percentages, concluding that 50% Matrigel yielded the most optimal results.

-The generation and maintenance of CRC organoids were discussed. Five lines of organoids were generated using three types of samples: (1) Localized tumoral and surrounding non-tumoral organoids [2 lines], (2) Metastatic colon organoids [1 line], (3) Rectum organoids [2 lines].

-Morphological characterization of the organoids was carried out to verify that they were reliable models of the disease. These analyses were performed using Immunohistochemistry, Immunofluorescence, and Hematoxylin & Eosin staining.

-Molecular characterization of tumoral tissue and corresponding tissue-derived organoids by Next Generation Sequencing using a customized panel was performed. It showed that the generated organoids mimicked the genetic profile of the tumoral tissue, hence reflecting the traits of each patient.

-Lastly, a drug assay was optimized using localized tumor organoids. Sensitivity to different treatments based on viability changes was evaluated. It was the first step towards the corroboration that the effects observed in organoids reflected the response of the patient. In the future, the analysis of organoids' sensitivity to different treatments could be extrapolated to the clinic improving the survival of the patients.

## 6. REFERENCES

- AHMAD, A. A.; WANG, Y.; GRACZ, A. D.; SIMS, C. E.; MAGNESS, S. T.; & ALLBRITTON, N. L. (2014). Optimization of 3-D organotypic primary colonic cultures for organ-on-chip applications. *Journal of Biological Engineering*, 8(1), 9. <https://doi.org/10.1186/1754-1611-8-9>
- BENVENUTI, S.; SARTORE-BIANCHI, A.; DI NICOLANTONIO, F.; ZANON, C.; MORONI, M.; VERONESE, S.; SIENA, S., & BARDELLI, A. (2007). Oncogenic activation of the ras/raf signaling pathway impairs the response of metastatic colorectal cancers to anti-epidermal growth factor receptor antibody therapies. *Cancer Research*, 67(6), 2643-2648. <https://doi.org/10.1158/0008-5472.CAN-06-4158>
- BOJ, S. F.; HWANG, C.-I.; BAKER, L. A.; CHIO, I. I. C.; ENGLE, D. D.; CORBO, V.; JAGER, M.; PONZ-SARVISE, M.; TIRIAC, H.; SPECTOR, M. S.; GRACANIN, A.; ONI, T.; YU, K. H.; VAN BOXTEL, R.; HUCH, M.; RIVERA, K. D.; WILSON, J. P.; FEIGIN, M. E.; ÖHLUND, D.; ... TUVESON, D. A. (2015). Organoid models of human and mouse ductal pancreatic cancer. *Cell*, 160(1-2), 324-338. <https://doi.org/10.1016/j.cell.2014.12.021>
- BROGUIERE, N.; ISENMANN, L.; HIRT, C.; RINGEL, T.; PLACZEK, S.; CAVALLI, E.; RINGNALDA, F.; VILLIGER, L.; ZÜLLIG, R.; LEHMANN, R.; ROGLER, G.; HEIM, M. H.; SCHÜLER, J.; ZENOBI-WONG, M., & SCHWANK, G. (2018). Growth of epithelial organoids in a defined hydrogel. *Advanced Materials*, 30(43), 1801621. <https://doi.org/10.1002/adma.201801621>
- BROUTIER, L.; MASTROGIOVANNI, G.; VERSTEGEN, M. M.; FRANCIES, H. E.; GAVARRÓ, L. M.; BRADSHAW, C. R.; ALLEN, G. E.; ARNES-BENITO, R.; SIDOROVA, O.; GASPERSZ, M. P.; GEORGAKOPOULOS, N.; KOO, B.-K.; DIETMANN, S.; DAVIES, S. E.; PRASEEDOM, R. K.; LIESHOUT, R.; IJZERMANS, J. N. M.; WIGMORE, S. J.; SAEB-PARSY, K.; ... HUCH, M. (2017). Human primary liver cancer-derived organoid cultures for disease modeling and drug screening. *Nature Medicine*, 23(12), 1424-1435. <https://doi.org/10.1038/nm.4438>
- CANCER GENOME ATLAS NETWORK (2012). Comprehensive molecular characterization of human colon and rectal cancer. *Nature*, 487(7407), 330–337. <https://doi.org/10.1038/nature11252>
- CLEVERS, H. (2016). Modeling Development and Disease with Organoids. *Cell*, 165(7), 1586-1597. <https://doi.org/10.1016/j.cell.2016.05.082>
- CLINICALTRIALS.GOV (n.d.) *Search of: Cancer organoid - List Results*. Viewed May 15th, 2020. Retrieved from, <https://clinicaltrials.gov/ct2/results?cond=cancer+organoid&term=&cntry=&state=&city=&dist=>
- DEKKER, E.; TANIS, P. J.; VLEUGELS, J. L. A.; KASI, P. M., & WALLACE, M. B. (2019). Colorectal cancer. *The Lancet*, 394(10207), 1467-1480. [https://doi.org/10.1016/S0140-6736\(19\)32319-0](https://doi.org/10.1016/S0140-6736(19)32319-0)
- DIJKSTRA, K. K.; CATTANEO, C. M.; WEEBER, F.; CHALABI, M.; VAN DE HAAR, J.; FANCHI, L. F.; SLAGTER, M.; VAN DER VELDEN, D. L.; KAING, S.; KELDERMAN, S.; VAN ROOIJ, N.; VAN LEERDAM, M. E.; DEPLA, A.; SMIT, E. F.; HARTEMINK, K. J.; DE GROOT, R.; WOLKERS, M. C.; SACHS, N.; SNAEBJORNSSON, P.; ... VOEST, E. E. (2018). Generation of tumor-reactive t cells by co-culture of peripheral blood lymphocytes and tumor organoids. *Cell*, 174(6), 1586-1598.e12. <https://doi.org/10.1016/j.cell.2018.07.009>
- DROST, J., & CLEVERS, H. (2018). Organoids in cancer research. *Nature Reviews Cancer*, 18(7), 407-418. <https://doi.org/10.1038/s41568-018-0007-6>
- FAN, H.; DEMIRCI, U., & CHEN, P. (2019). Emerging organoid models: Leaping forward in cancer research. *Journal of Hematology & Oncology*, 12(1), 142. <https://doi.org/10.1186/s13045-019-0832-4>
- FLORESCU-TENEA R.M., & KAMAL, A.M. (2019). Colorectal cancer: An update on treatment options and future perspectives. *Current Health Sciences Journal*, 2, 134-141. <https://doi.org/10.12865/CHSJ.45.02.02>
- FUJII, E.; YAMAZAKI, M.; KAWAI, S.; OHTANI, Y.; WATANABE, T.; KATO, A., & SUZUKI, M. (2018). A simple method for histopathological evaluation of organoids. *Journal of Toxicologic Pathology*, 31(1), 81-85. <https://doi.org/10.1293/tox.2017-0060>

- FUJII, M.; SHIMOKAWA, M.; DATE, S.; TAKANO, A.; MATANO, M.; NANKI, K.; OHTA, Y.; TOSHIMITSU, K.; NAKAZATO, Y.; KAWASAKI, K.; URAOKA, T.; WATANABE, T.; KANAI, T. & SATO, T. (2016). A colorectal tumor organoid library demonstrates progressive loss of niche factor requirements during tumorigenesis. *Cell Stem Cell*, 18(6), 827-838. <https://doi.org/10.1016/j.stem.2016.04.003>
- FUMAGALLI, A.; DROST, J.; SUIJKERBUIJK, S. J. E.; VAN BOXTEL, R.; DE LIGT, J.; OFFERHAUS, G. J.; BEGTHEL, H.; BEERLING, E.; TAN, E. H.; SANSOM, O. J.; CUPPEN, E.; CLEVERS, H., & VAN RHEENEN, J. (2017). Genetic dissection of colorectal cancer progression by orthotopic transplantation of engineered cancer organoids. *Proceedings of the National Academy of Sciences*, 114(12), E2357-E2364. <https://doi.org/10.1073/pnas.1701219114>
- GAO, D., & CHEN, Y. (2015). Organoid development in cancer genome discovery. *Current Opinion in Genetics & Development*, 30, 42-48. <https://doi.org/10.1016/j.gde.2015.02.007>
- GAO, D.; VELA, I.; SBONER, A.; IAQUINTA, P. J.; KARTHAUS, W. R.; GOPALAN, A.; DOWLING, C.; WANJALA, J. N.; UNDVALL, E. A.; ARORA, V. K.; WONGVIPAT, J.; KOSSAI, M.; RAMAZANOGLU, S.; BARBOZA, L. P.; DI, W.; CAO, Z.; ZHANG, Q. F.; SIROTA, I.; RAN, L., ... CHEN, Y. (2014). Organoid cultures derived from patients with advanced prostate cancer. *Cell*, 159(1), 176-187. <https://doi.org/10.1016/j.cell.2014.08.016>
- GRANDORI, C., & KEMP, C. J. (2018). Personalized cancer models for target discovery and precision medicine. *Trends in Cancer*, 4(9), 634-642. <https://doi.org/10.1016/j.trecan.2018.07.005>
- GUENOT, D.; GUÉRIN, E.; AGUILLON-ROMAIN, S.; PENCREACH, E.; SCHNEIDER, A.; NEUVILLE, A.; CHENARD, M.-P.; DULUC, I.; DU MANOIR, S.; BRIGAND, C.; OUDET, P.; KEDINGER, M., & GAUB, M.-P. (2006). Primary tumour genetic alterations and intra-tumoral heterogeneity are maintained in xenografts of human colon cancers showing chromosome instability. *The Journal of Pathology*, 208(5), 643-652. <https://doi.org/10.1002/path.1936>
- GUINNEY, J.; DIENSTMANN, R.; WANG, X.; DE REYNIÈS, A.; SCHLICKER, A.; SONESON, C.; MARISA, L.; ROEPMAN, P.; NYAMUNDANDA, G.; ANGELINO, P.; BOT, B. M.; MORRIS, J. S.; SIMON, I. M.; GERSTER, S.; FESSLER, E.; DE SOUSA E MELO, F.; MISSIAGLIA, E.; RAMAY, H.; BARRAS, D.; ... & TEJPAR, S. (2015). The consensus molecular subtypes of colorectal cancer. *Nature Medicine*, 21(11), 1350-1356. <https://doi.org/10.1038/nm.3967>
- INAMURA, K. (2018). Colorectal cancers: An update on their molecular pathology. *Cancers*, 10(1), 26. <https://doi.org/10.3390/cancers10010026>
- KAMB, A. (2005). What's wrong with our cancer models? *Nature Reviews Drug Discovery*, 4(2), 161-165. <https://doi.org/10.1038/nrd1635>
- KAMBUROV, A.; LAWRENCE, M. S.; POLAK, P.; LESHCHINER, I.; LAGE, K.; GOLUB, T. R.; LANDER, E. S. & GETZ, G. (2015). Comprehensive assessment of cancer missense mutation clustering in protein structures. *Proceedings of the National Academy of Sciences*, 112(40), E5486-E5495. <https://doi.org/10.1073/pnas.1516373112>
- KLEINMAN, H. K., & MARTIN, G. R. (2005). Matrigel: Basement membrane matrix with biological activity. *Seminars in Cancer Biology*, 15(5), 378-386. <https://doi.org/10.1016/j.semcancer.2005.05.004>
- KOCER, B.; SORAN, A.; ERDOGAN, S.; KARABEYOGLU, M.; YILDIRIM, O.; EROGLU, A.; BOZKURT, B., & CENGIZ, O. (2002). Expression of MUC5AC in colorectal carcinoma and relationship with prognosis. *Pathology International*, 52(7), 470-477. <https://doi.org/10.1046/j.1440-1827.2002.01369.x>
- KWONG, L. N., & DOVE, W. F. (2009). APC and its modifiers in colon cancer. *Advances in experimental medicine and biology*, 656, 85-106. [https://doi.org/10.1007/978-1-4419-1145-2\\_8](https://doi.org/10.1007/978-1-4419-1145-2_8)
- LI, M., & IZPISUA BELMONTE, J. C. (2019). Organoids—Preclinical models of human disease. *New England Journal of Medicine*, 380(6), 569-579. <https://doi.org/10.1056/NEJMra1806175>
- LIBANJE, F.; RAINGEAUD, J.; LUAN, R.; THOMAS, Z.; ZAJAC, O.; VEIGA, J.; MARISA, L.; ADAM, J.; BOIGE, V.; MALKA, D.; GOÉRÉ, D.; HALL, A.; SOAZEC, J.; PRALL, F.; GELLI, M.; DARTIGUES, P., & JAULIN, F. (2019). rock 2 inhibition triggers the collective invasion of colorectal adenocarcinomas. *The EMBO Journal*, 38(14). <https://doi.org/10.15252/embj.201899299>

- MATANO, M.; DATE, S.; SHIMOKAWA, M.; TAKANO, A.; FUJII, M.; OHTA, Y.; WATANABE, T.; KANAI, T., & SATO, T. (2015). Modeling colorectal cancer using CRISPR-Cas9-mediated engineering of human intestinal organoids. *Nature Medicine*, 21(3), 256-262. <https://doi.org/10.1038/nm.3802>
- MCGRANAHAN, N., & SWANTON, C. (2017). Clonal heterogeneity and tumor evolution: Past, present, and the future. *Cell*, 168(4), 613-628. <https://doi.org/10.1016/j.cell.2017.01.018>
- NAGLE, P. W.; PLUKKER, J. TH. M.; MUIJS, C. T.; VAN LUIJK, P., & COPPES, R. P. (2018). Patient-derived tumor organoids for prediction of cancer treatment response. *Seminars in Cancer Biology*, 53, 258-264. <https://doi.org/10.1016/j.semcancer.2018.06.005>
- NAKAYAMA, M., & OSHIMA, M. (2019). Mutant p53 in colon cancer. *Journal of Molecular Cell Biology*, 11(4), 267-276. <https://doi.org/10.1093/jmcb/mjy075>
- NOJADEH, J. N.; BEHROUZ SHARIF, S.; & SAKHINIA, E. (2018). Microsatellite instability in colorectal cancer. *EXCLI Journal*, 17, 159-168. <https://doi.org/10.17179/excli2017-948>
- NUSSRAT, F. L.; ALI, H. H.; HUSSEIN, H. G., & AL-UKASHI, R. J. (2011). Immunohistochemical expression of ki-67 and p53 in colorectal adenomas: A clinicopathological study. *Oman Medical journal*, 229-234. <https://doi.org/10.5001/omj.2011.57>
- ONUMA, K.; OCHIAI, M.; ORIHASHI, K.; TAKAHASHI, M.; IMAI, T.; NAKAGAMA, H.; & HIPPO, Y. (2013). Genetic reconstitution of tumorigenesis in primary intestinal cells. *Proceedings of the National Academy of Sciences*, 110(27), 11127-11132. <https://doi.org/10.1073/pnas.1221926110>
- PEREZ, R. O.; BRESCIANI, B. H.; BRESCIANI, C.; PROSCURSHIM, I.; KISS, D.; GAMA-RODRIGUES, J.; PEREIRA, D. D.; RAWET, V.; CECCONNELLO, I., & HABR-GAMA, A. (2008). Mucinous colorectal adenocarcinoma: Influence of mucin expression (Muc1, 2 and 5) on clinico-pathological features and prognosis. *International Journal of Colorectal Disease*, 23(8), 757-765. <https://doi.org/10.1007/s00384-008-0486-0>
- ROTH, A. D.; TEJPAR, S.; DELORENZI, M.; YAN, P.; FIOCCA, R.; KLINGBIEL, D.; DIETRICH, D.; BIESMANS, B.; BODOKY, G.; BARONE, C.; ARANDA, E.; NORDLINGER, B.; CISAR, L.; LABIANCA, R.; CUNNINGHAM, D.; VAN CUTSEM, E. & BOSMAN, F. (2010). Prognostic role of *kras* and *braf* in stage ii and iii resected colon cancer: Results of the translational study on the petacc-3, eortc 40993, sakk 60-00 trial. *Journal of Clinical Oncology*, 28(3), 466-474. <https://doi.org/10.1200/JCO.2009.23.3452>
- SACHS, N., & CLEVERS, H. (2014). Organoid cultures for the analysis of cancer phenotypes. *Current Opinion in Genetics & Development*, 24, 68-73. <https://doi.org/10.1016/j.gde.2013.11.012>
- SACHS, N.; DE LIGT, J.; KOPPER, O.; GOGOLA, E.; BOUNOVA, G.; WEEBER, F.; BALGOBIND, A. V.; WIND, K.; GRACANIN, A.; BEGTHEL, H.; KORVING, J.; VAN BOXTEL, R.; DUARTE, A. A.; LELIEVELD, D.; VAN HOECK, A.; ERNST, R. F.; BLOKZIJL, F.; NIJMAN, I. J.; HOOGSTRAAT, M., ... CLEVERS, H. (2018). A living biobank of breast cancer organoids captures disease heterogeneity. *Cell*, 172(1-2), 373-386.e10. <https://doi.org/10.1016/j.cell.2017.11.010>
- SATO, T.; STANGE, D. E., FERRANTE, M.; VRIES, R. G. J.; VAN ES, J. H.; VAN DEN BRINK, S.; VAN HOUTDT, W. J.; PRONK, A.; VAN GORP, J.; SIERSEMA, P. D., & CLEVERS, H. (2011). Long-term expansion of epithelial organoids from human colon, adenoma, adenocarcinoma, and barrett's epithelium. *Gastroenterology*, 141(5), 1762-1772. <https://doi.org/10.1053/j.gastro.2011.07.050>
- SATO, T.; VRIES, R. G., SNIPPERT, H. J.; VAN DE WETERING, M.; BARKER, N., STANGE, D. E., VAN ES, J. H., ABO, A., KUJALA, P., PETERS, P. J., & CLEVERS, H. (2009). Single Lgr5 stem cells build crypt-villus structures in vitro without a mesenchymal niche. *Nature*, 459(7244), 262-265. <https://doi.org/10.1038/nature07935>
- SCHUTGENS, F., & CLEVERS, H. (2020). Human organoids: Tools for understanding biology and treating diseases. *Annual Review of Pathology: Mechanisms of Disease*, 15(1), 211-234. <https://doi.org/10.1146/annurev-pathmechdis-012419-032611>
- SIEGEL, R. L.; MILLER, K. D., & JEMAL, A. (2020). Cancer statistics, 2020. *CA: A Cancer Journal for Clinicians*, 70(1), 7-30. <https://doi.org/10.3322/caac.21590>

- SKARDAL, A.; SHUPE, T. & ATALA, A. (2016). Organoid-on-a-chip and body-on-a-chip systems for drug screening and disease modeling. *Drug Discovery Today*, 21(9), 1399-1411. <https://doi.org/10.1016/j.drudis.2016.07.003>
- TENTLER, J. J.; TAN, A. C.; WEEKES, C. D.; JIMENO, A.; LEONG, S.; PITTS, T. M.; ARCAROLI, J. J.; MESSERSMITH, W. A., & ECKHARDT, S. G. (2012). Patient-derived tumour xenografts as models for oncology drug development. *Nature Reviews Clinical Oncology*, 9(6), 338-350. <https://doi.org/10.1038/nrclinonc.2012.61>
- VELLINGA, T. T.; DEN UIL, S.; RINKES, I. H. B.; MARVIN, D.; PONSIOEN, B.; ALVAREZ-VARELA, A.; FATRAI, S.; SCHEELE, C.; ZWIJNENBURG, D. A.; SNIPPERT, H.; VERMEULEN, L.; MEDEMA, J. P.; STOCKMANN, H. B.; KOSTER, J.; FIJNEMAN, R. J. A.; DE ROOIJ, J. & KRANENBURG, O. (2016). Collagen-rich stroma in aggressive colon tumors induces mesenchymal gene expression and tumor cell invasion. *Oncogene*, 35(40), 5263-5271. <https://doi.org/10.1038/onc.2016.60>
- VLACHOGIANNIS, G.; HEDAYAT, S.; VATSIU, A.; JAMIN, Y.; FERNÁNDEZ-MATEOS, J.; KHAN, K.; LAMPIS, A.; EASON, K.; HUNTINGFORD, I.; BURKE, R.; RATA, M.; KOH, D.-M.; TUNARIU, N.; COLLINS, D.; HULKKI-WILSON, S.; RAGULAN, C.; SPITERI, I.; MOORCRAFT, S. Y.; CHAU, I., ... VALERI, N. (2018). Patient-derived organoids model treatment response of metastatic gastrointestinal cancers. *Science*, 359(6378), 920-926. <https://doi.org/10.1126/science.aao2774>
- WANG, H.; JIN, S.; LU, H.; MI, S.; SHAO, W.; ZUO, X.; YIN, H.; ZENG, S.; SHIMAMOTO, F. & QI, G. (2017). Expression of survivin, MUC2 and MUC5 in colorectal cancer and their association with clinicopathological characteristics. *Oncology Letters*, 14(1), 1011-1016. <https://doi.org/10.3892/ol.2017.6218>
- WORLD HEALTH ORGANIZATION. (2018). Cancer. Viewed on May 15<sup>th</sup>; retrieved from <https://www.who.int/news-room/fact-sheets/detail/cancer>
- XU, Z.; GAO, Y.; HAO, Y.; LI, E.; WANG, Y.; ZHANG, J.; WANG, W.; GAO, Z., & WANG, Q. (2013). Application of a microfluidic chip-based 3D co-culture to test drug sensitivity for individualized treatment of lung cancer. *Biomaterials*, 34(16), 4109-4117. <https://doi.org/10.1016/j.biomaterials.2013.02.045>
- YU, F.; HUNZIKER, W. & CHOUDHURY, D. (2019). Engineering microfluidic organoid-on-a-chip platforms. *Micromachines*, 10(3), 165. <https://doi.org/10.3390/mi10030165>

## 7. APPENDIX

**Supplementary table 1. List of biobanks generated from multiple cancer types.** Collections can be generated from both primary tumors and metastases for some of the cancer types. Number of organoid lines that were characterized per biobank are represented along with the histological subtypes. References in the table correspond to the references from the original article. Image taken from Schutgens & Clevers, 2020.

Organ of origin	Number of lines <sup>a</sup>	Histological subtypes	Reference
Colon	22	Adenocarcinomas	22
Colorectum	55	Premalignant lesions (tubular and tubulovillous adenomas, sessile serrated lesions, and a hyperplastic polyp) Adenocarcinomas (well differentiated, moderately differentiated, poorly differentiated, mucinous, not specified) Metastases of adenocarcinomas Neuroendocrine carcinomas	79
Colorectum	10	Colorectal metastases	78
Rectum (for cystic fibrosis)	71	Not applicable	23
Pancreas	8	Ductal adenocarcinomas	19
Pancreas	39	Ductal adenocarcinomas	80
Pancreas	114	Ductal adenocarcinomas	82
Liver	8	Hepatocellular carcinomas Cholangiocarcinomas Combined hepatocellular cholangiocarcinomas	86
Bladder	20	Urothelial carcinomas Squamous cell carcinomas	
Prostate	7	Adenocarcinoma metastases and circulating tumor cells	76
Ovary	33	High-grade serous carcinoma	28
Ovary	56	Borderline tumors (both mucinous and serous) Clear cell carcinomas Endometrioid carcinomas Mucinous carcinomas Low-grade serous carcinomas High-grade serous carcinomas	85
Breast	95	Ductal carcinoma Lobular carcinoma	32
Mixed <sup>b</sup>	56	Tumors from prostate, breast, colorectal, esophagus, brain, pancreas, lung, small intestine, ovary, uterus, soft tissue (not further specified), bladder, ureter, kidney	87
Mixed	<sup>c</sup>	Metastatic colorectal cancer Metastatic gastroesophageal cancer	83

<sup>a</sup>Refers to the number of organoid lines reported, not the number of patients (for some patients, multiple lines were established).

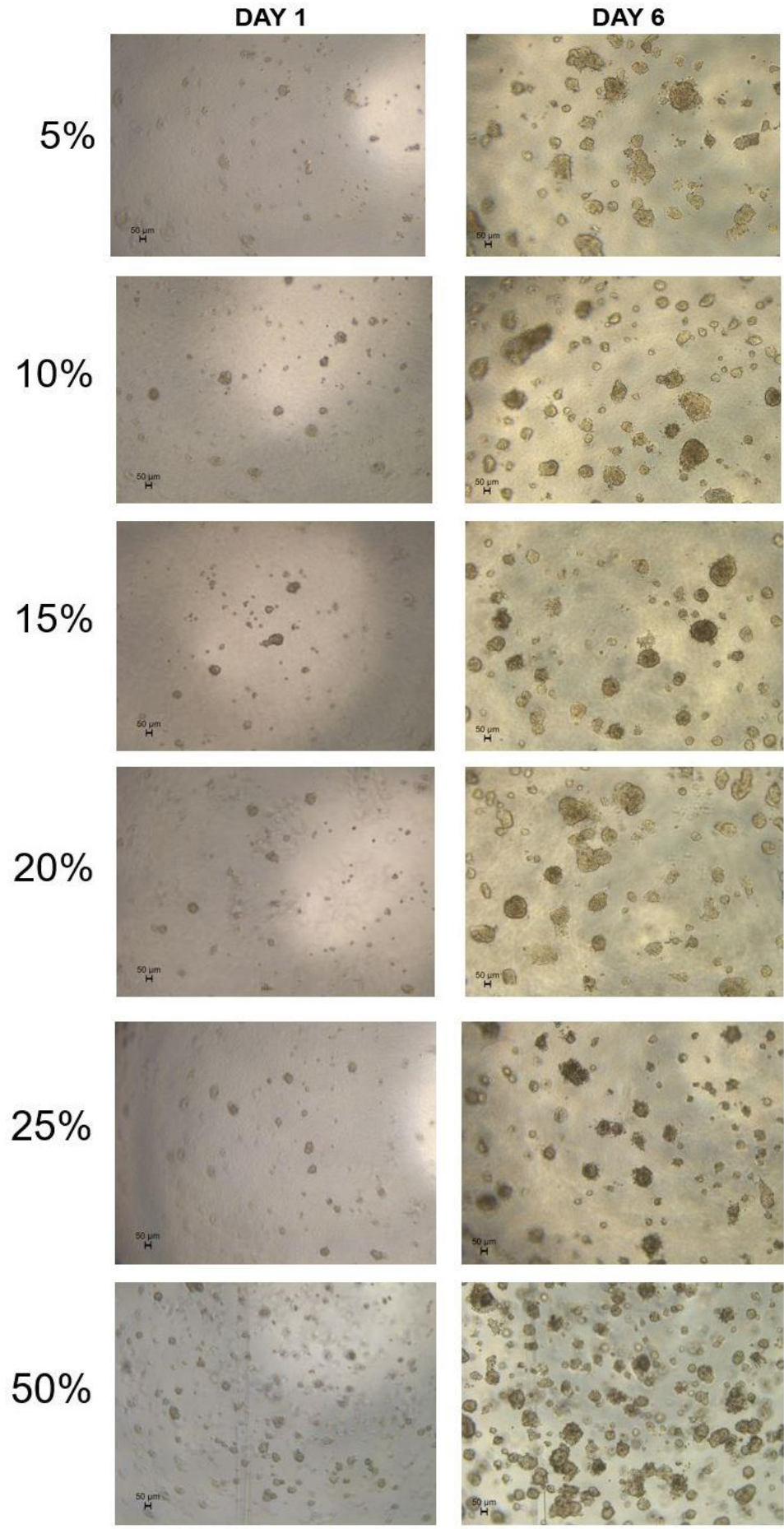
<sup>b</sup>Histological types were not comprehensively reported.

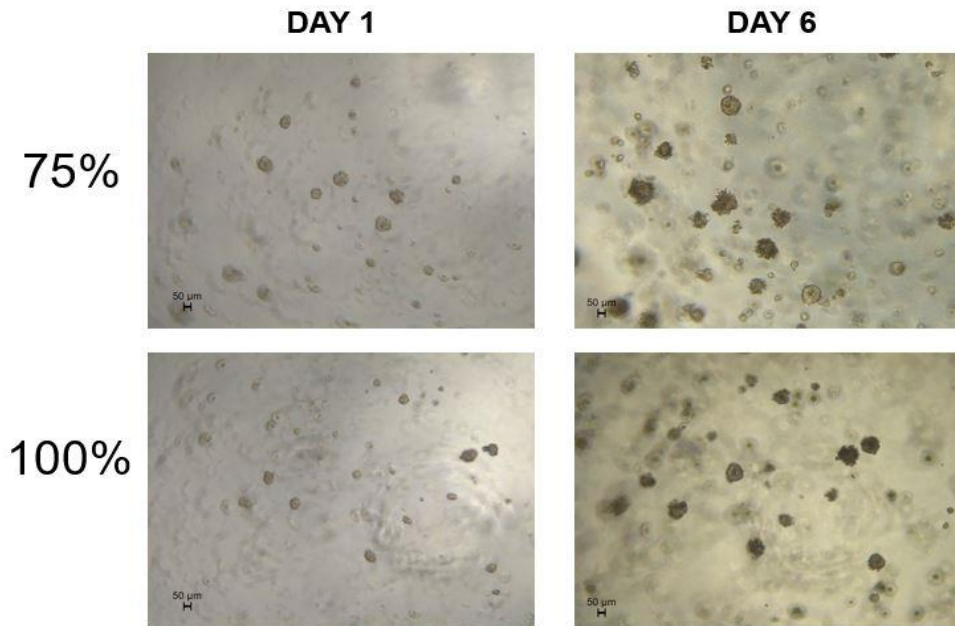
<sup>c</sup>The number of lines was not specifically mentioned (83).

	1	2	3	4	5	6	7	8	9	10	11	12
A												
B		Control	0.1 $\mu$ M	1 $\mu$ M	5 $\mu$ M	10 $\mu$ M	50 $\mu$ M	100 $\mu$ M	150 $\mu$ M	200 $\mu$ M	Blank	
C		Control	0.1 $\mu$ M	1 $\mu$ M	5 $\mu$ M	10 $\mu$ M	50 $\mu$ M	100 $\mu$ M	150 $\mu$ M	200 $\mu$ M	Blank	
D		Control	0.1 $\mu$ M	1 $\mu$ M	5 $\mu$ M	10 $\mu$ M	50 $\mu$ M	100 $\mu$ M	150 $\mu$ M	200 $\mu$ M	Blank	
E		Control	0.1 $\mu$ M	1 $\mu$ M	5 $\mu$ M	10 $\mu$ M	50 $\mu$ M	100 $\mu$ M	150 $\mu$ M	200 $\mu$ M	Blank	
F		Control	0.1 $\mu$ M	1 $\mu$ M	5 $\mu$ M	10 $\mu$ M	50 $\mu$ M	100 $\mu$ M	150 $\mu$ M	200 $\mu$ M	Blank	
G		Control	0.1 $\mu$ M	1 $\mu$ M	5 $\mu$ M	10 $\mu$ M	50 $\mu$ M	100 $\mu$ M	150 $\mu$ M	200 $\mu$ M	Blank	
H												

	1	2	3	4	5	6	7	8	9	10	11	12
A												
B		Control	0.1 $\mu$ M	1 $\mu$ M	5 $\mu$ M	10 $\mu$ M	50 $\mu$ M	100 $\mu$ M	150 $\mu$ M	200 $\mu$ M	Blank	
C		Control	0.1 $\mu$ M	1 $\mu$ M	5 $\mu$ M	10 $\mu$ M	50 $\mu$ M	100 $\mu$ M	150 $\mu$ M	200 $\mu$ M	Blank	
D		Control	0.1 $\mu$ M	1 $\mu$ M	5 $\mu$ M	10 $\mu$ M	50 $\mu$ M	100 $\mu$ M	150 $\mu$ M	200 $\mu$ M	Blank	
E												
F												
G												
H												

**Supplementary figure 1. Schematic representation of the distribution of drugs: 5-FU and Oxaliplatin independently and as a combination.** Due to the number of wells required per condition, two plates had to be used. The response to the treatment was analyzed for each drug independently in P96W 1 and as a combination in P96W 2. For both plates the first and last rows and columns were left empty. The second column was used as control and the eleventh column was used as blank. Grey means that it was empty, yellow was for wells containing 5-FU, blue was for wells containing Oxaliplatin and green was for the combination of 5-FU and Oxaliplatin





**Supplementary figure 2. Colorectal cancer tumoral organoids (CTO65-P02) cultured in different Matrigel concentrations for the evaluation of the growth rate.** All wells contained a final volume of 5  $\mu\text{L}$  and 1000 cells/ $\mu\text{L}$  were seeded. Pictures were taken on day 1 and day 6 of culture. Scale bar: 50  $\mu\text{m}$ ; 5X magnification was used. Matrigel concentrations were indicated in the picture